

Development of a Flexible Pavement Design Protocol for the UAE Based  
on the Mechanistic-Empirical Pavement Design Guide

BY

Ammar Alalkim Alzaabi

Presented to the Office of Graduate Studies at the  
University of Texas at Arlington

In Partial Fulfillment of the Requirements

For the Degree of

Doctor of Philosophy (Ph.D.)

December 2019

Copyright ©

All Rights Reserved



Ammar Alalkim Alzaabi 2019

## **Acknowledgements**

I would like to express my sincere gratitude to my supervisor Dr. Stefan Romanoschi, who was always available when I needed his guidance or assistance. Our discussions went beyond the pavement engineering realm and I am forever indebted for the time he dedicated to share his experience and wisdom. I would also like to thank my committee members, Dr. Victoria Chen, Dr. Suyun Ham, Dr. James Williams for their insightful remarks and support.

I would also like to extend my thankfulness to the Ministry of Infrastructure Development, starting with the Minister H.E. Dr. Abdullah Belhaif Al Nuaimi for overseeing a research supporting environment. I would also extend my gratitude to Dr. Daniel Llort, who managed the data supply process and ensured that all my requirements were met.

I would like to thank my beloved parents for supporting my ambitions. Your love, wisdom and guidance will be never overseen. My thanks also go to my siblings and friends, your indirect contributions will not be forgotten.

Lastly but not least, a special thank you goes to my other half, my wife, and son for being part of my research experience. They have supported me through thick and thin and were always there to lift me on my low days. Our memories during this phase of our lives will always be cherished.

## **Abstract**

Development of a Flexible Pavement Design Protocol for the UAE Based on the Mechanistic-Empirical Pavement Design Guide

Ammar Alalkim Alzaabi

The University of Texas at Arlington, 2019

Supervising Professor: Dr. Stefan Romanoschi

The Ministry of Infrastructure Development in the UAE has used the AASHTO 1993 Pavement Design Guide for the design of new flexible pavement structures for many years. An improved pavement design method, called the Mechanistic-Empirical Pavement Design Guide (MEPDG) was developed by AASHTO in their effort to update the empirical method used in 1993 Guide. The project was initiated by the National Cooperative Highway Research Program (NCHRP) 1-37A project. It is based on mechanistic-empirical analysis of the pavement structure to predict the performance of the pavements subject to pavement structure and materials, traffic and environmental conditions.

The development allowed for more complex design concepts. The design approach used is different because the pavement design engineers can determine the damage sustained over the design life and changes of ride quality over time and thus adjust their design to serve specific requirements. Due to the advanced models used, the MEPDG is expected to be adopted for use in the United Arab Emirates in the near future. In order to improve the performance prediction of the models a local calibration is

required to accommodate the local pavement materials, traffic characteristics and the environmental conditions.

The objective of this study was to calibrate the latest version of the MEPDG, the AASHTOWare Pavement ME 2.5.5 software program to the local conditions of UAE. To achieve this, twenty flexible pavement sections were selected for the calibration process. The structural configuration, in-situ pavement performance, traffic and climate data was obtained from the Ministry of Infrastructure Development. AASHTOWare Pavement ME software runs were made using the nationally calibrated coefficients and the predicted rutting and IRI values were compared with measured values. The difference between the measured and the predicted distresses were minimized through calibration of the rutting and IRI models. A new set of local calibration coefficients ( $\beta_{r1}$ ,  $\beta_{GB}$ , and  $\beta_{SG}$ ) for the rutting in the asphalt concrete, base and subgrade layer models were obtained. The calibration of IRI was done by deriving the appropriate model coefficients ( $C1$  and  $C4$ ) for the total rutting and the Site Factor. No calibration was conducted for the fatigue alligator cracking and transverse cracking since they very rarely develop in UAE pavement. However, the rutting and the roughness models were successfully calibrated.

## Table of Contents

1.	Chapter 1: Introduction, Problem Statement and Objectives.....	1
1.1	Introduction.....	1
1.2	Problem Statement.....	3
1.3	Objectives.....	5
1.4	Research Approach.....	5
2.	Chapter 2: Literature Review.....	7
2.1	AASHTO Pavement Design History.....	7
2.2	Mechanistic Empirical Pavement Design Guide (MEPDG) Method.....	10
2.3	Ministry of Infrastructure Development Threshold Criteria.....	15
2.4	Pavement Performance and Prediction Models for Flexible Pavement.....	17
2.4.1	Load Related Cracking Model - Alligator Cracking Model (Bottom-up Fatigue).....	18
2.4.2	Load Related Cracking Model - Longitudinal Cracking Model (Top-Down).....	21
2.4.3	Non-Load Related Cracking Model-Transverse Cracking.....	22
2.4.4	Permanent Deformation Model (Rutting).....	24
2.4.5	Asphalt Concrete Layer Model.....	25
2.4.6	Unbound Materials Model.....	26
2.4.7	International Roughness Index Model (IRI).....	27
2.5	Calibration Efforts of the MEPDG to Accustom Local Conditions.....	29
3.	Chapter 3: Data Collection and Methodology.....	35
3.1	Hierarchical Input Levels.....	35
3.2	Data Collection Process.....	36
3.2.1	Data Components.....	37
3.2.2	Selection of Pavement Sections.....	44
3.3	Criteria for MEPDG Pavement Design.....	46
3.4	Pavement Materials Data.....	53
3.4.1	Asphalt Concrete Volumetric Properties.....	54
3.4.2	Unbound Layer Properties.....	55
3.4.3	Subgrade Layer Properties.....	56
3.5	Traffic Data.....	57
3.6	Climate Data Assembling.....	60
4.	Chapter 4: Local Calibration and Validation Plan.....	63

4.1 Developing the Performance Models for Ministry of Infrastructure Development .....	64
4.2 Local Bias Assessment .....	64
4.3 Conduct local calibration to determine transfer functions .....	66
4.4 Performance Models Validation .....	67
5. Chapter 5: Development of Local Calibration Models.....	68
5.1 Assess Local Bias for Global Calibration.....	68
5.2 Eliminate Local Bias of Performance Models .....	72
5.2.1 Elimination of Local Bias for Permanent Deformation Model .....	73
5.2.2 Elimination of Local Bias for IRI Model.....	85
5.3 Goodness of Fit Statistics.....	91
6. Chapter 6 Summary, Conclusion and Recommendations.....	93
6.1 Summary and Conclusion.....	93
6.2 Recommendations.....	95
7. References.....	97
8. Acronyms .....	101
9. Appendix A – Pavement Distress Data Sets .....	102
10. Appendix B Material Properties .....	105
11. Appendix C – Traffic Distribution.....	108

## List of Tables

Table 2-1 NCHRP projects supporting implementation and adoption of MEPDG .....	9
Table 2-2 Summary of local calibration factors for flexible pavements by Arizona state agency .....	30
Table 2-3 Criteria to Determine Model Adequacy for Colorado Conditions .....	31
Table 2-4 Summary of local calibration factors for flexible pavements by CDOT .....	31
Table 2-5 Summary of local calibration factors for flexible pavements by Georgia DOT .....	32
Table 2-6 Results of US States Local Calibrations .....	33
Table 3-1 Climate Parameters Inputs .....	41
Table 3-2 Traffic parameters inputs .....	41
Table 3-3 Asphalt concrete material properties inputs .....	42
Table 3-4 Base material properties inputs .....	42
Table 3-5 Subgrade material properties inputs .....	43
Table 3-6 Roadway classification and structural layer thicknesses .....	43
Table 3-7 Measured Distress Values .....	50
Table 3-8 Statistical Summary for Distress Values of Investigated Sections .....	50
Table 3-9 Base, Subbase gradation information was provided by MOID .....	55
Table 5-1 Criteria for Adequacy of Global Model .....	68
Table 5-2 Condition Survey Date in Months .....	69
Table 5-3 Bias Statistical Analysis Using Global Calibration .....	70
Table 5-4 Sum of Squared Error Computations .....	74
Table 5-5 Local Calibration Coefficients .....	74
Table 5-6 Computation of Calibration Coefficient $\beta_{1r}$ .....	76
Table 5-7 Computation of Calibration Coefficient $\beta_{s1GB}$ .....	77
Table 5-8 Computation of Calibration Coefficient $\beta_{s1SG}$ .....	78
Table 5-9 Computation of Total Rutting Using Global Calibration .....	79
Table 5-10 Computation of Total Rutting Using Local Calibration .....	80
Table 5-11 Local Calibration Coefficients .....	86
Table 5-12 Sum of Squared Error Computations .....	87
Table 5-13 Computation of IRI Using Global and Local Calibrations .....	88
Table 5-14 Computation of Site Factor .....	89
Table 5-15 Mean Error and SEE for Global and Local Calibration .....	92



## List of Figures

Figure 2-1 Mechanistic Empirical Design Methodology.....	13
Figure 2-2 MOID IRI, Rutting, Cracks Comparison Charts.....	16
Figure 3-1 Condition Survey Equipment.....	37
Figure 3-2 Data requirements for ME Design .....	38
Figure 3-3 Map of U.A.E: Road Network in Northern Emirates from the Ministry of Infrastructure Development .....	45
Figure 3-4 Map of E18-2 .....	45
Figure 3-5 Map of E311 .....	46
Figure 3-6 Map of E-99 .....	46
Figure 3-7 Map of E18-1 .....	46
Figure 3-8 E99 Construction Dates Input.....	48
Figure 3-9 Distress Threshold Criteria and Inputs.....	48
Figure 3-10 Longitudinal Cracking vs. Time Plot .....	51
Figure 3-11 Rutting vs. Time Plot .....	52
Figure 3-12 IRI vs. Time Plot .....	52
Figure 3-13 Asphalt layer inputs.....	54
Figure 3-14 Non Stabilized Base Input .....	56
Figure 3-15 Subgrade Gradation and properties Input.....	57
Figure 3-16 Traffic Inputs.....	58
Figure 3-17 FHWA Vehicle Classification.....	59
Figure 3-18 Vehicle Classification Distribution and Growth Input.....	60
Figure 3-19 Climate Data Selection .....	61
Figure 3-20 Climate Data Computations .....	62
Figure 4-1 Improvement in Bias and Precision.....	65
Figure 5-1 Total Measured Rutting vs Total predicted Rutting in Global Calibration.....	71
Figure 5-2 Measured IRI vs Predicted IRI based on Global Calibration .....	72
Figure 5-3 Asphalt Layer (Global Calibration) .....	81
Figure 5-4 Asphalt Layer Rutting (Local Calibration) .....	81
Figure 5-5 Base Layer Rutting (Global Calibration) .....	82
Figure 5-6 Base Layer Rutting (Local Calibration) .....	82
Figure 5-7 Subgrade Layer Rutting (Global Calibration) .....	83
Figure 5-8 Subgrade Layer Rutting (Local Calibration).....	83
Figure 5-9 Total Rutting (Global Calibration).....	84
Figure 5-10 Total Rutting (Local Calibration) .....	84
Figure 5-11 Total Rutting vs Residual Error .....	85
Figure 5-12 IRI (Global Calibration).....	90
Figure 5-13 IRI (Local Calibration).....	90
Figure 5-14 IRI vs. Residual Error.....	91

## **Chapter 1: Introduction, Problem Statement and Objectives**

### **1.1 Introduction**

The United Arab Emirates is a developing nation striving to construct and maintain a civil infrastructure that continuously competes to become the best in the World. The Ministry of Infrastructure Development which is the Governmental branch overseeing, constructing and managing these assets, has set ambitious targets for the U.A.E to maintain its global status as an economic powerhouse in the region. By having a well maintained, holistic infrastructure system, the Government believes it can attract international investors. Therefore, the Ministry has set very strict targets that would trigger maintenance requirements for different types of deteriorations in the UAE's road network.

The ministry has conducted research to compare with benchmark values set by developed nations such as Norway, Finland, Germany, Australia and the U.S. State of California. These nations are amongst the richest in the world, in terms of GDP and GDP per capita.

The lifecycle cost of pavement maintenance needs to be managed as it could easily exceed a nation's economic capacity. As nations expand, research centers and stakeholders in the civil infrastructure market aspire to develop and adopt economically sustainable approaches to maintain their infrastructure asset systems at high standards. An example of a struggle to maintain the set benchmarks, is the United States. In a recent study conducted by the American Society of Civil Engineers (ASCE), the United States infrastructure has received an overall rating of D+, despite that the U.S. remains the biggest economy in the world. Roads have received a rating of D, "frequently in poor condition and chronically underfunded" as described in the report (ASCE 2017). The report elaborates in mentioning

that a mile in every five miles of U.S. roads required immediate attention and those rehabilitation requirements keep backlogging.

The MEPDG was developed by AASHTO in their effort to update the empirical method used in 1993 AASHTO Design Guide. The development allowed for more complex design requirements, that would be hard to apply to an empirical method based on road tests. MEPDG's design of the pavement structure is assumed in a trial procedure, where a software computes the trial design's response to stresses from load applications and environmental factors. This allows pavement engineers to determine damage sustained over the design life and changes of ride quality over time and thus adjust to serve their design purpose.

It will serve as an improvement to the UAE's current use of the empirical 1993 AASHTO Design Guide. It is a more comprehensive pavement design and analysis tool, which allows for a forensic analysis through its iterative process in distress prediction based on design inputs, saving time and money. It allows for the optimization of the design features, rather than the conventional approach of increasing pavement thickness when there's an anticipated load increase. The design procedure gives the ability to quantify the accuracy of the predicted outcomes, based on design specifications implemented.

The MEPDG will assist in achieving the UAE's goal by providing for more resilient, economically sustainable pavement. This should ultimately reduce the life cycle cost of pavements, allowing the UAE to preserve precious funds for future generation, without compromising the pavement condition throughout its road network. The objective of this research is to calibrate the performance models in AASHTO Pavement ME to local conditions of the U.A.E.

## **1.2 Problem Statement**

Pavement design plays a significant role in economic sustainability in countries worldwide. A proper pavement design prolongs pavements life cycle, leading to savings in maintenance, rehabilitation and even construction of new pavements. Thus, the custodians of road networks have been overseeing and funding pavement design improvements and advances; producing more accurate design methods that accommodate broader spectrums of design attributes, covering more relevant factors, resulting in resilient and sustainable pavements. An improvement of 1% in the life of pavements due to better design process could lead to savings in the excess of 150 million dollars annually in the United States.

The United Arab Emirates (UAE) has been utilizing the American Association of State Highway and Transportation Officials (AASHTO) empirical design method until 2010, when they decided to review the method adopted, examine other pavement design methods utilized worldwide and conclude into choosing what's best for the UAE. Due to rapid economic growth, heavier trucks have been used causing accelerated pavement damage which has reduced the service life of the road network. These increasing traffic demands need to be addressed with a more efficient design method that takes into account the traffic influx and the climate. The whole aim of the exercise was to select a pavement design method that was created based on similar environmental conditions of the UAE, without compromising the technical and financial aspects.

In recent years, more attention has been given to the study of pavement response to certain damage accumulation and reasons for distress. Hence pavement design methods have incorporated the mechanistic aspect of design into the widely implemented empirical design methods. So rather than basing designs on pavement performance observations, an

actual examination of the reasons behind distresses and failures is included. There are two important performance criteria that would reduce rutting and fatigue cracking. The vertical compressive strain is the cause for rutting while the horizontal tensile strain at the bottom of the Hot Mix Asphalt (HMA) layer, is the cause for structural fatigue. The advancement in software and hardware devices have allowed for enhanced computational capabilities, allowing the development and use of complex design algorithms and methodologies.

This improvement has become possible due to the advancement in pavement design software, that enhanced the accuracy in distress prediction capability. The software performs complex stress, strain and deflection analysis with the inclusion of different factors in the form of traffic data, design data, performance data and climate data. The estimated values are compared against threshold distress values in order to define pavement failure. This will allow for a better characterization the different factors and how they influence the performance of a particular pavement design.

The implementation effort requires an extensive array of input data, which must represent the specific local conditions such as, materials characteristics, traffic and climatic data as well as performance requirements. Moreover, the performance models will be calibrated for the state, region or country the models will be used for in order to improve the efficiency of the design process. This is because of large variation in traffic, climatic conditions, pavement configurations and construction quality from one region or state to another.

### **1.3 Objectives**

The aim of this project is to:

- Calibrate the performance models of flexible pavement distresses in AASHTOWare Pavement ME 2.5.5 to the local conditions of the United Arab Emirates.
- Establish a database for historical pavement performance and MEPDG data that can be used for a future calibration, if needed.

### **1.4 Research Approach**

The dissertation will be organized into five chapters. Chapter 1 contains the introduction, aim and objectives of this dissertation. Chapter 2 describes and explain previous research that has been conducted in relation to MEPDG Calibration for local conditions, pavement condition surveying and management, pavement distresses and pavement design. The case studies will focus on areas with similar conditions to those of the UAE and their approach to MEPDG adoption. Chapter 3 discusses the methodological approach utilized based on the available resources. The chapter explains the different data input level for MEPDG data and which level was utilized for the research and reasons for it. There will also be a detailed description of the data collection process, the types of data and the amount of data collected. The tools administered to derive this data from both the researcher and the local agency is touched upon. Chapter 4 covers the statistical analysis of the data in terms of carrying out by performing local bias estimations to determine the reliability of the data. Chapter 5 describes the calibration work of the dissertation, where transfer functions are developed, assisting the ministry to design using MEPDG, utilizing

calibrated transfer functions. Chapter 6 contains the conclusions derived from this research as well as the recommendations to enhance future contributions to the study.

## **Chapter 2: Literature Review**

### **2.1 AASHTO Pavement Design History**

The AASHTO Pavement Design Guide was developed in 1972 to serve as an empirical design tool, for both, rigid and flexible pavements. This project was initiated in 1958 by constructing road test segments in the state of Illinois, funded by the American Association of State Highway Officials (AASHTO). The purpose of this project was to test a variety of pavement structures against different traffic axle loads and configurations. Six loops of various pavement sections were constructed, with uniform mix designs and one kind of subgrade soil. These tests helped quantify the deterioration and damage caused due to the sustained truck impact. A number of improved versions were published throughout the years, the most recent being in 1993 and were adopted by states and countries worldwide.

The design of a pavement by evaluating the performance of specific road sections; after experiencing traffic and weather conditions in a set period of time, is an empirical design method. In contrast, the modelling of a pavement's structural layers as multi-layered elastic systems and computing stresses and strain at critical locations in the pavement is a mechanistic design method.

The MEPDG was developed by AASHTO in their effort to update the empirical method used in 1993 AASHTO Design Guide. The development allowed for more complex design requirements, that would be hard to apply to a method based on road tests. The design approach used is different because the design is carried out in reverse. Contrary to the empirical method, the design of the pavement structure is assumed in a trial procedure, where an MEPDG software computes the trial design's response to stresses from load applications and environmental factors. This allows pavement



engineers to determine damage sustained over the design life and changes of ride quality over time and thus adjust to serve their design purpose. While conventionally, a simple design procedure would be conducted, where various design inputs are selected to establish the design requirements of the pavement.

The capability to accumulate damage on a monthly basis over the entire design period, is a precedent in pavement design achieved by MEPDG. This approach allows for the simulation of damage occurrence in pavements, load by load, over monthly intervals. Elastic moduli are used to determine change in the pavement within representative intervals.

Another major improvement when comparing the two design methods is the more comprehensive outlook of traffic load in the M-E method, when compared to the AASHTO 1993 Guide. In the latter method, Equivalent Axle Load (ESAL) is used to characterize traffic, while the former includes full axle load spectrum traffic inputs to calculate the configuration, magnitude, and traffic loading frequency. This enhances the accuracy to determine the axle loads that are going to be applied on the pavement, in intervals, by calculating damage accumulation, incrementally.

The implementation of MEPDG is a tedious process which requires an array of data inputs and several challenges that need to be overcome by different agencies that are considering its utility. These are laid out in the NCHRP 1-37A (National Cooperative Highway Research Program) report and are summarized as follows:

- Determining data requirements for design inputs, how they shall be collected and establishing a database for inputs;
- Determining the performance and reliability design criteria;

- Assessing availability of testing equipment required;
- Acquiring computer hardware and software requirements;
- Established a database for all existing projects, including new and rehabilitated pavements;
- Conducting local calibration and validation of performance models;
- Establish training requirements for respective pavement design staff;

Since 2002, several NCHRP projects have been commissioned to support the implementation and adoption of MEPDG in the United States. These are listed periodically in table (2-1)

Project Number	Project Title
NCHRP 01-37	Development of the 2002 guide for the design of new and rehabilitated pavement structures
NCHRP 01-39	Traffic Data collection, analysis and forecasting for mechanistic pavement design
NCHRP 01-40A	Independent review of the recommended mechanistic-empirical design guide and software
NCHRP 01-40B	User manual and local calibration guide for the M-E pavement guide and software
NCHRP 01-40D	Technical assistance to NCHRP project 1-40A: versions 0.9 and 1.0 of the M-E pavement design software
NCHRP 01-41	Models for predicting reflection cracking of hot-mix asphalt overlays
NCHRP 01-42A	Models for predicting top-down cracking of hot-mix asphalt layers
NCHRP 01-47	Sensitivity evaluation of MEPDG performance prediction
NCHRP 01-48	Incorporating pavement preservation into the MEPDG
NCHRP 01-50	Quantifying the Influence of geosynthetics on pavement performance
NCHRP 09-30	Experimental plan for calibration and validation of HMA performance models for mix and structural design

*Table 2-1 NCHRP projects supporting implementation and adoption of MEPDG*

AASHTOWare Pavement ME is the most up to date version of the software product of the AASHTO MEPDG. It was initially released in 2007 as a result of the National Cooperative Highway Research Program (NCHRP 1-40D) as indicated in table 2-1 and has undergone wide review. Version 2.5.5. is the latest version, which was issued in April 2019 incorporating both new climate data and different aspects of traffic loadings. Axle load distributions and traffic counts are computed in parallel with different climate attributes to allow for the adjustment of the stiffness of structural layers, at different periods of the design life. Through this computation and the recalibration of AASHTOWare performance models to suit local conditions, accurate predictions of distresses are produced. This increases the reliability of the outcome, yielding cost effective design solutions that would result in more resilient pavements. MEPDG adoptions are expanding throughout the U.S. and worldwide for the design of new flexible pavements.

## **2.2 Mechanistic Empirical Pavement Design Guide (MEPDG) Method**

The MEPDG method was developed to design and evaluate new and rehabilitated pavement structures. The structural responses of a pavement in the form of deflections, stresses and strains are determined mechanistically after computing, pavement layer thickness, material properties, traffic loads and climatic conditions. Those responses are used to estimate the magnitude of several models. There are two types of empirical models incorporated in the MEPDG method used for flexible pavements:

1. The prediction the distress directly from the pavement response, which is used to calculate rut depth.

2. The comparison between the predicted distress and the measured distress, which is used for fatigue cracking.

For a specific state, region or country, the empirical distress models need to be calibrated with condition surveys' data to achieve accurate prediction models.

The MEPDG design procedure comprises of three main stages. Firstly, the input values are developed, where the responsible agency establishes potential design strategies and an analysis of the foundation is conducted. Additionally, various inputs are collected and a database is established. The second stage involves the performance analysis by carrying out the initial trial design. Pavement performance models are used to analyse the trial design by calculating the pavement response, incrementally, over time. The pavement response analysis includes cumulative smoothness and distresses over time. Subsequently, a comparison is carried out between the predicted outcomes of the initial trial design and the design criteria at a specified reliability level, as per the requirements of the responsible agency. This process is iterative and hence a repetition of the procedure may be required until all the design requirements are met. The final stage involves considering alternatives by assessing engineering attributes and conducting life cycle cost analyses.

In this form of design, there are three significant stages in building the design model that incorporates the mechanistic feature of the software. These are the evaluation stage, followed by the analysis stage. Initially, input levels are prepared, comprising foundation analysis, rehabilitated projects function, deflection testing and back-calculations for the evaluation of existing pavements. The foundation analysis incorporates stiffness determination, freeze thaw phenomenon, assessing volume change and also investigating

drainage issues. While rehabilitated projects function takes into account subgrade analysis and the extent of the distresses being investigated, detecting potential causes for those distresses. The development of pavement materials' characterizations and traffic load assessments follow the stress and strain calculations. Finally, a climatic model analyses the environmental effects (i.e. temperature and precipitation) on every layer of the pavement structure. It also covers, windspeed, sunlight and water-table. Moreover, the software allows the user to indicate the pavement design life anticipated and the thresholds for each distress criteria, based on a preferred reliability level.

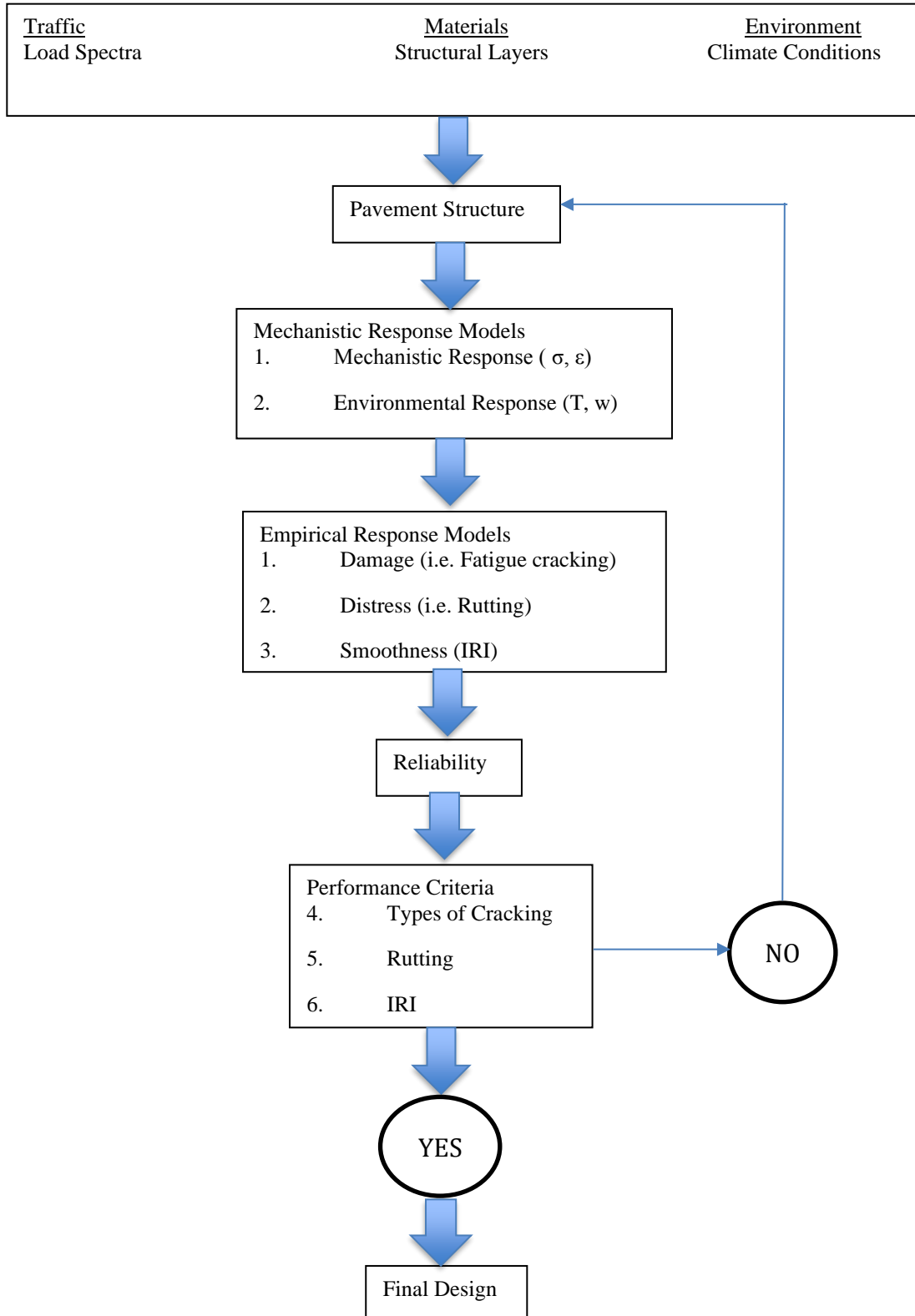


Figure 2-1 Mechanistic Empirical Design Methodology

As presented in Figure 2-1, the analysis starts with a trial design of a certain pavement. It requires inputs from the design related to structure thickness and material properties for all layers. These include the Asphalt concrete layer, Base layer (also sub-base) and subgrade layer. The initial IRI of the pavement, right after construction must be inputted. The software then analyses the trial design over the design period (more than 20 years). The traffic load calculations and climatic condition effects, using the mentioned analysis models, yield pavement distress models. The software produces an analysis report of the outcome on the trial design with magnitude estimated of distresses (IRI, rutting and cracking) over the entire design period. If the distresses at the end of the design life are higher than those set as design criteria, adjustments must be made to the design by reviewing the structure design and material properties. This process could be repeated until an acceptable design is achieved. The accuracy of MEPDG design is based on the reliability of the design inputs and the accuracy of the prediction models.

MEPDG sets a reliability level that is user-defined for each distress type. It is the probability that the pavement will have higher distresses than the user set distress thresholds at the end of pavement design life. It can be expressed as:

$$\textit{Reliability} = \textit{Probability} ( \textit{Predicted Distress} < \textit{Critical Distress} )$$

Equation (1)

The model assumes that the error of all the distresses affecting the pavement are normally distributed, with predicted mean and a standard deviation values for each distress. This is translated in the reliability formula:

$$D_{reliability} = D_{mean} + S_d * z_r$$

Equation (2)

Where:

$D_{reliability}$  is the distress value at a reliability, r (between 50% and 99.9%)

$D_{mean}$  is the distress using 50% reliability

$S_d$  is the standard deviation for the distress

$z_r$  is the normal deviate from the normal distribution corresponding to reliability r

The final stage is called the Strategic Selection stage, which takes into account the non-technical attributes of a design project and rather the political and economical aspect. It reviews the lifecycle cost analysis of the selected pavement design and whether it is economically viable for the responsible entity. It is also channelled by policy issues of governing bodies and internal managerial decisions. These could trigger a different engineering design and construction approach.

### **2.3 Ministry of Infrastructure Development Threshold Criteria**

In order to perform a design using the MEPDG software, the threshold criteria for each distress is required. The Ministry has set very strict targets that would trigger maintenance requirements for different types of deteriorations in the UAE's road network. These targets are reflected in the benchmarks set for the values of IRI, Rutting and Cracking, as shown in figure 2-2





### COMPARISON CHART

#### CONDITION SURVEY

Limit values on each parameter

For maintained roads

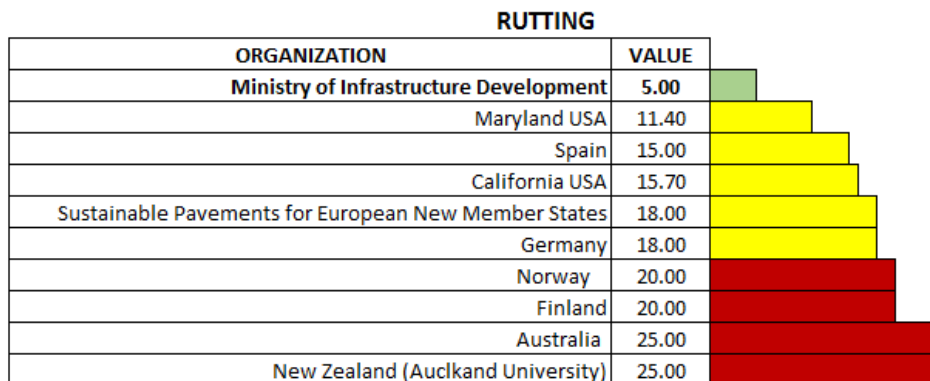
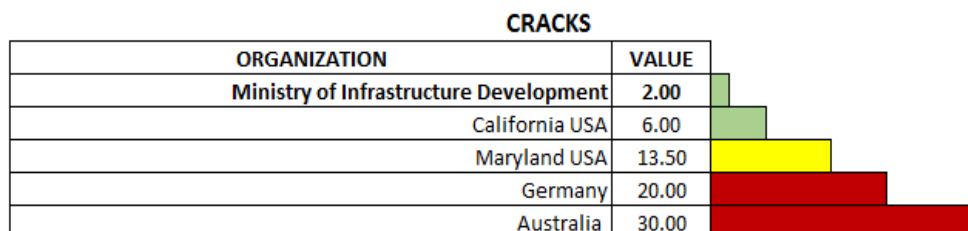
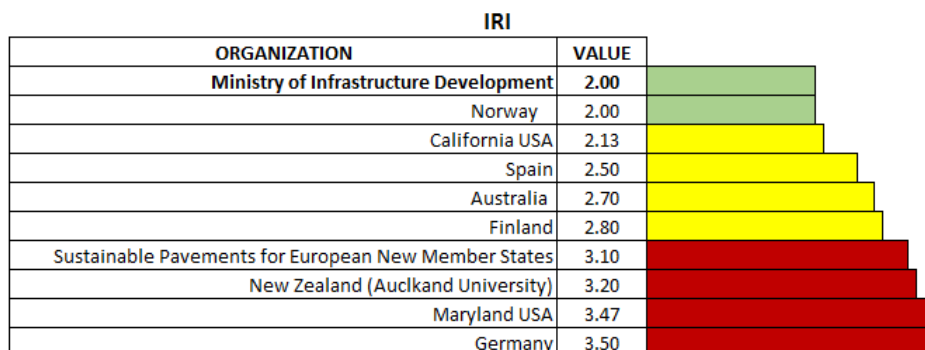


Figure 2-2 MOID IRI, Rutting, Cracks Comparison Charts

## **2.4 Pavement Performance and Prediction Models for Flexible Pavement**

MEPDG calibration requires materials data, traffic data and climatic data. MEPDG further divides the pavement structure layer and foundation into sub-layers to determine pavement response. The thickness of these sub-layers is based on the: material used, the layer thickness and the depth with the pavement structure (Maupin 2006). A modified form of the linear elastic theory program called JULEA, incorporated in the AASHTO MEPDG software, predicts a pavement response in each sub-layer. There are two pavement response models incorporated into the MEPDG software, one predicts responses due to traffic loading and the other predicts the climatic effects on the pavement structure.

The first response model utilized is the Multi-Layer Elastic Theory (MLET), which utilizes the JULEA algorithm to compute different axle configurations by superposition formulation. To perform the load related analysis, layer thickness, modulus of elasticity and Poisson's ratio need to be defined for each layer. It also requires a computation of tire pressure and contact area. Structural responses in critical locations are estimated using the maximum damage calculations based on the computed traffic load. The response is evaluated in critical points within each layer and the highest value is used to predict the performance of the pavement. The critical points are determined by the type of distress being evaluated:

- Rutting requires an evaluation of dynamic and permanent vertical compressive strains at mid depth, top of subgrade and 15.2 cm into the subgrade.
- Fatigue cracking requires an evaluation of horizontal tensile strain at the

surface, 1.3cm into the Asphalt layer and at the bottom of the Asphalt layer.

The second model is the Enhanced Integrated Climatic Model (EICM), which is used to calculate the average temperature and moisture conditions within the pavement. This is used to determine the dynamic modulus in each asphalt-layer and the resilient modulus in granular material (AASHTO 2008). The EICM model is also used in the thermal cracking prediction model to compute temperature distributions within the layers. It also calculates the resilient modulus by calculating adjustment factors based on the moisture content predicted in the base and the subgrade for each 2-week period. By factoring freeze-thaw cycles, the resilient modulus is also adjusted, where it is greater at freezing and lower at thawing.

#### **2.4.1 Load Related Cracking Model - Alligator Cracking Model (Bottom-up Fatigue)**

The two types of fatigue cracking that could be experienced in asphalt pavements are: top-down cracking or bottom-up cracking. Cracking is either, identified on the surface, 1.3cm into the surface layer or at the bottom of the surface HMA layer (Witczak 2004). These are defined as follows:

1. The tensile strain at the bottom of the asphalt layer which represents the asphalt fatigue
2. The tensile strain at the bottom of the cemented material, resembling the cement material fatigue.

It is calculated by predicting the damage which is then translated into the area of crack extension. MEPDG utilized the Asphalt Institute's method of Fatigue crack calculation.

According to AASHTO (2010) a reasonable Standard Error of Estimate (SEE) for alligator cracking is 7%.

Initially, the number of axle load repetitions to failure for a certain strain magnitude is calculated:

$$N_{f-HMA} = k_{f1}(C)(C_H)\beta_{f1}(\varepsilon_t)^{\beta_{f2} k_{f2}} (E_{HMA})^{\beta_{f3} k_{f3}}$$

Equation (3)

Where:

$N_{f-HMA}$  is the number of allowable axle load repetitions on a HMA pavement

$k_{f1}, k_{f2}, k_{f3}$  are global calibration coefficients calculated using the LTPP database.

$$k_{f1}=0.007566, k_{f2}= -3.9492, k_{f3}= -1.281$$

$E_{HMA}$  is the asphalt concrete stiffness / dynamic modulus of HMA

$\varepsilon_t$  is the tensile strain at the critical location within the Asphalt layer

$\beta_{f1}, \beta_{f2}, \beta_{f3}$  are the local calibration coefficients assumed to have a value of 1.

$C$  is the adjustment factor based on laboratory testing

$C_H$  is the thickness correction factor depending on the crack type

The Thickness Correction Factor for alligator cracking is:

$$C_H = \frac{1}{0.000398 + \frac{0.003602}{1 + e^{(11.02 - 3.49 * h_{AC})}}}$$

Equation (4)

Where:

$h_{AC}$  is the total Asphalt layer thickness

The adjustment factor laboratory field is calculated using:

$$C = 10^M$$

Equation (5)

$$M = 4.84 \left( \frac{V_{beff}}{V_a + V_{beff}} - 0.69 \right)$$

Equation (6)

Where:

$V_a$  is the air voids % in the HMA mixture

$V_{beff}$  is the % of binder content by volume

Miner's Law is applied to calculate the incremental damage from given Load (number of repetitions), using the below formula:

$$D = \sum_{i=1}^T \frac{n_i}{N_{f-HMA}}$$

Equation (7)

Where:

$D$  is % damage

$T$  is the total number of 2-week periods (26 per year)

$n_i$  is the actual number of axle load repetitions for period (i)

$N_{f-HMA}$  is the number of allowable axle load repetitions on a HMA pavement for period (i)

Finally, the prediction of Alligator cracking extent is calculated as:

$$FC_{Bottom} = \left( \frac{C_4}{1 + e^{(C_1 C'_1 + C_2 C'_2 * \log_{10}(D * 100))}} \right) * \left( \frac{1}{60} \right)$$

Equation (8)

$$C'_2 = -2.40874 - 39.748(1 + h_{AC})^{-2.856}$$

Equation (9)

$$C'_1 = -2C'_2$$

Equation (10)

Where:

$FC_{Bottom}$  is fatigue cracking based on % of total area

$D$  is % damage

$C_1, C_2, C_4$  are global calibration coefficients calculated using the LTPP database

$C_1 = 1.0, C_2 = 1$  and  $C_4 = 6000$

$h_{AC}$  is the total Asphalt layer thickness (mm)

$\frac{1}{60}$  Is to convert square feet to % of alligator cracking

#### **2.4.2 Load Related Cracking Model - Longitudinal Cracking Model (Top-Down)**

Longitudinal cracks are a form of fatigue cracking, which occur parallel to the centerline of the pavement and are not necessarily a consequence of a structural incapacity. It depends on the location of the crack and where it extends on the pavement. The cracks initiate at the surface as short longitudinal cracks and with continuous truck loadings, the cracks become connected. The unit for longitudinal cracking is ft/mi or m/km. AASHTO (2010) determines that a reasonable Standard SEE would be 600 ft/mi.

Initially, the number of axle load repetitions to failure for a certain strain magnitude is calculated using Equation 3. The adjustment factor laboratory field is calculated using Equations 5 and 6.

The conversion of Top-Down Fatigue Damage into Longitudinal fatigue cracking is calculated using:

$$FC_{Top} = 10.56 \left( \frac{C_4}{1 + e^{(C_1 - C_2 * \log_{10} D)}} \right)$$

Equation (11)

Where:

$FC_{Top}$  is longitudinal cracking (m/km)

$D$  is % damage

$C_1, C_2, C_4$  are global calibration coefficients calculated using the LTPP database

$$C_1 = 7.0, C_2 = 3.5 \text{ and } C_4 = 1000$$

10.56 is to convert from ft per 500ft into ft/mile

The Thickness Correction Factor for longitudinal cracking is:

$$C_H = \frac{1}{0.01 + \frac{12.00}{1 + e^{(15.676 - 2.8186 h_{AC})}}}$$

Equation (12)

Where:

$h_{AC}$  is the total Asphalt layer thickness

### **2.4.3 Non-Load Related Cracking Model-Transverse Cracking**

The difference in thermal change between the different layers of the pavement causes cracking at the surface. Characteristically, the crack extends across the width of the

pavement in a transverse manner. The cause of this is due to the failure in tension of the asphalt cracking at the bottom of the surface layer. The crack propagation for a given thermal cycle is calculated using Paris Law:

$$\Delta C = A * \Delta K^n$$

Equation (12)

Where:

$\Delta C$  is the change in depth of crack per thermal cycle

$\Delta K$  is the change in stress intensity factor during a thermal cycle

A, n are fracture parameters of the HMA

$$n = 0.8 \left( 1 + \frac{1}{m} \right)$$

Equation (13)

$$A = 10^{k_t \beta_t [4.389 - 2.52 * \log(E_{HMA} * \sigma_m * n)]}$$

Equation (14)

Where:

$k_t$  is the coefficient estimated by global calibration for;

level 1 = 1.5, level 2 = 0.5 and level 3 = 1.5

$\beta_t$  is the local calibration parameters

M m-value from the indirect tensile creep compliance curve

$E_{HMA}$  is the indirect tensile modulus of the HMA (psi)

$\sigma_m$  is the tensile strength of the HMA (psi)

The length of Thermal cracking predicted in relation to crack depth to % of cracking is calculated using:



$$TC = \beta_1 * N\left(\frac{\log\left(\frac{C_d}{h_{ac}}\right)}{\sigma}\right)$$

Equation (15)

Where:

$TC$  is the predicted thermal cracking in ft/mile

$\beta_1$  is the coefficient estimated by global calibration = 400

$N$  is the standard normal distribution evaluated at  $[z]$

$C_d$  is the depth of the crack (in)

$h_{ac}$  is the thickness of the Asphalt layer (in)

$\sigma$  is the standard deviation of the log of the depth of cracks (for the global calibration = 0.769) (in)

#### **2.4.4 Permanent Deformation Model (Rutting)**

According to Selvaraj (2007) the general cause of rutting is slow moving traffic, bearing heavy loads, in areas with hot climates conditions. It is the main reason for pavement distress in the UAE. Shear deformation occurs in the surface asphalt layer of the pavement, underneath the loading area. This results in densification around the area of the load, thus producing a depression the pavement level in areas where the pressure is high and hence, due to the thermal visco-elasto-plastic behavior of asphalt concrete, a permanent deformation of the pavement develops. The compressive strain at the top of the subgrade also causes rutting. Ayres (1997) and Kaloush (2001) have modified Leahy's empirical model to predict the rutting degree of the Asphalt layer of the pavement. For the unbound materials layer, Ayres (1997) has modified Tseng and Lytton's rutting prediction model

(1989), which was further improved in 2004 by El-Basyouny and Witczak. A reasonable SEE for rutting is 0.10in.

To calculate the total rut depth for all layers, the following formula is used:

$$\Delta\rho_{total} = \Delta\rho_{AC} + \Delta\rho_{base} + \Delta\rho_{soil}$$

(Equation 16)

#### **2.4.5 Asphalt Concrete Layer Model**

Computation of total estimated rut depth incorporating sublayers of AC layer

$$\Delta\rho_{AC} = \sum_{i=1}^n \varepsilon_{P(HMA)} * h_{HMA} = \beta_{1r} k_z \varepsilon_{r(HMA)} 10^{k_{1r}} N^{k_{2r}} \beta_{2r} T^{k_{3r}} \beta_{3r}$$

(Equation 17)

Where:

$\Delta\rho_{AC}$  is the permanent deformation at the Asphalt Layer

$\sum^n$  is the number of sublayers

$\varepsilon_{P(HMA)}$  is the vertical plastic strain at mid-depth of layer (i)

$h_{HMA}$  is the thickness of the sublayer (i)

$\varepsilon_{r(HMA)}$  is the computed elastic strain at mid-depth of sublayer (i)

T is the temperature of the pavement mixture ( $^{\circ}F$ ) at mid depth of sublayer (i)

N is the number of repetitions for a given load

$k_z$  is the depth of the correction factor

$k_{1r}, k_{2r}, k_{3r}$  are global calibration coefficients determined by laboratory testing

$$k_{1r} = -3.35412, k_{2r} = 0.4791, k_{3r} = 1.5606$$

$\beta_{1r}, \beta_{2r}, \beta_{3r}$  are local calibration coefficients

The depth correction factor quantifies pressures at different depths using the following equations:

$$k_z = (C_1 + C_2 * depth) * 0.328196^{depth}$$

(Equation 18)

$$C_1 = -0.1039 * (h_{AC})^2 + 2.4868 * h_{AC} - 17.342$$

(Equation 19)

$$C_2 = 0.0172 * (h_{AC})^2 - 1.7331 * h_{AC} + 27.428$$

(Equation 20)

Where:

$depth$  is the depth to where the maximum strain is calculated (in)

$h_{AC}$  is the thickness of the Asphalt layer (mm)

#### **2.4.6 Unbound Materials Model**

Permanent deformation at a certain sublayer, equations 21, 22, 23 and 24:

$$\Delta\rho_{soil} = \beta_{s1} k_{s1} \left(\frac{\varepsilon_0}{\varepsilon_r}\right) e^{-\left(\frac{\rho}{N}\right)^\beta} \varepsilon_v h_{soil}$$

Equation (21)

Where:

$\Delta\rho_{soil}$  is the permanent deformation for sublayer (i)

$\beta_{s1}$  is the local calibration coefficient for the base or the subgrade

$k_{s1}$	is the global calibration coefficient 1.673 for granular materials and 1.35 for fine grained materials
$\varepsilon_0$	is the intercept determined by laboratory testing
$\varepsilon_r$	is the resilient strain obtained by laboratory testing
$\varepsilon_v$	is the computed elastic strain at mid-depth of sublayer (i) for a certain load
N	is the number of repetitions for a given load
$h_{soil}$	is the thickness of the unbound sublayer (i)

$$\log \beta = -0.61119 - 0.017638 * W_c$$

Equation (22)

$$\rho = 10^9 \left[ \frac{0.0075}{(1 - (10^9)^\beta)} \right]^{\frac{1}{\beta}}$$

Equation (23)

Where:

$W_c$  is the % water content

#### **2.4.7 International Roughness Index Model (IRI)**

IRI stands for the International Roughness Index, a measure of longitudinal smoothness of the pavement surface. Surface irregularities develop after the pavement has been opened to traffic. The surface deforms either due to traffic action, or due to continuous climatic exposure. IRI is highly correlated with ongoing pavement distresses in the form of cracking or rutting (Bhattacharya 2015).

The IRI model values are computed as:

$$IRI = IRI_0 + C_1(RD) + C_2(FC_{Total}) + C_3(TC) + C_4(SF)$$

Equation (25)

Where:

$IRI_0$  is the initial IRI right after construction

$FC_{Total}$  is the area of all fatigue cracking as a % of the total area

$TC$  is the length of transverse cracking (m/km)

$RD$  is the average rut depth (mm)

$C_1, C_2, C_3, C_4$  are global calibration coefficients calculated using the LTPP database

$$C_1 = 40 \quad C_2 = 0.4 \quad C_3 = 0.008 \quad C_4 = 0.015$$

$SF$  is the site factor computed as:

$$SF = Age[0.02003(PI + 1) + 0.00794(Precip + 1) + 0.000636(FI + 1)]$$

Equation (26)

Where:

Age is the age of the pavement

PI is the plasticity index of the soil (%)

Precip is the average annual precipitation (in)

FI is the average annual freezing index ( $^{\circ}F$ )

## **2.5 Calibration Efforts of the MEPDG to Accustom Local Conditions**

The developers of the MEPDG have calibrated the models for the entire United States area, it was named the Global Calibration. The Global Calibration was done using the Long-Term Pavement Performance (LTPP) database, which comprises of:

1. Pavement Design and Material properties Data
2. Traffic Data
3. Climate Data

This was AASHTO's initial effort to conduct a nationwide Mechanistic Empirical Pavement Design Method. Therefore, in order to better suit a certain design condition, this data needs to be collected for the studied region. The calibration process constitutes an adjustment of the total error between the actual field data and the predicted data extrapolated from the MEPDG software, which uses the performance models explained earlier. For an accurate approach to calibration, extensive data is required for the local condition being investigated. This includes acquiring sets of data from LTPP for the local conditions. In other countries, a global database system is required to achieve local calibrations of the MEPDG. A calibration of the performance models using local conditions data is required to produce a more realistic prediction of distresses, for different areas that have different soil type and climatic conditions. A mathematical process is conducted to minimize total error or to minimize the difference between actual performance data and MEPDG computed performance data, by changing the model coefficients.

In a study carried out by Momin (2011) a simple linear regression was conducted to calibrate coefficient factors for the rutting model. These include coefficients for the Asphalt layer, subgrade and base. The Permanent deformation values were designated as the

independent variable in the calibration process. The local calibration coefficients were calculated as the inverse of the slope in the linear regression. The coefficients for cracking models (longitudinal and fatigue) were calibrated using the Microsoft Excel Solver. A MEPDG simulation was executed and the predicted values were compared with the actual cracking values. The sum of square of error (SSE) between the predicted values and the predicted and actual cracking data were minimized to obtain the calibration factor.

In 2014, the Arizona Department of Transport published their Local calibration report, which followed the Guide for Local Calibration of Mechanistic-Empirical Pavement Design Guide published by AASHTO in 2010. To gather the data, the Department used both LTPP and ADOT historical data to perform this calibration. They have also performed field surveys to verify the accuracy of the data and to complete any missing information. Their process of calibration was followed by a validation exercise, to ensure soundness of the results. The outcome for this exercise produced the below transfer functions for flexible pavements.

<b>Model</b>	<b>Model Coefficients</b>	<b>Calibration Factor</b>
<b>IRI</b>	C1	1.2281
	C2	0.1175
	C3	0.008
	C4	0.028
	SEE (in/mi)	8.7
<b>Fatigue Cracking</b>	$\beta_{f1}$	249.0087
	$\beta_{f2}$	1.00
	$\beta_{f3}$	1.2334
	SEE (%)	14.8
<b>Rutting</b>	$\beta_{r1}$	0.69
	$\beta_{b1}$ <i>Fine Graded</i>	0.37
	$\beta_{b1}$ <i>Granular</i>	0.14
	SEE (in)	0.11

Table 2-2 Summary of local calibration factors for flexible pavements by Arizona state agency

In 2009 Colorado Department of Transport (CDOT) started the data collection and input determination phase of their MEPDG adoption plan and between 2010 and 2011 they had created their input libraries and determined their local calibration values. A study was conducted in collaboration with a consultant (ARA) in 2013 to complete the local calibration efforts. A variety of new flexible pavement and overlay asphalt mix sections with different layer thickness were selected in their calibration effort. The location of these sections varied from hot to very cold areas. CDOT used a set of criteria to determine the adequacy of their calibration of the performance models as expressed in Table 2-3 below,

Criterion	Test Statistics	Model SEE	Rating
Goodness of Fit Test	Global HMA Alligator Cracking Model	<5	Good
		5 - 10	Fair
		>10	Poor
	Global HMA Total Rutting Model	<0.1 in	Good
		0.1-0.2 in	Fair
		>0.2 in	Poor
	Global HMA IRI Model	<19 in/mi	Good
		19-38 in/mi	Fair
		>38 in/mi	Poor
Bias	Hypothesis testing – Slope of linear measured vs. predicted distress model	p-value	Reject if p-value is <0.05
	Paired t-test between measured and predicted distress model	p-value	Reject if p-value is <0.05

Table 2-3 Criteria to Determine Model Adequacy for Colorado Conditions

Model	Model Coefficients	Calibration Factor
IRI	C1	35
	C2	0.3
	C3	0.02
	C4	0.019
	SEE (in/mi)	17.2
Fatigue Cracking	$\beta_{f1}$	130.367
	$\beta_{f2}$	1
	$\beta_{f3}$	1.218
	SEE (%)	9.4
Rutting	$\beta_{r1}$	0.3529
	$\beta_{b1}$	n/a
	$\beta_{s1}$	n/a
	SEE (in)	0.147

Table 2-4 Summary of local calibration factors for flexible pavements by CDOT



Georgia Department of Transport (GDOT) performed the local calibration of the MEPDG using LTPP and non-LTPP data for sites in the state. This was carried out to determine the local calibration factors for the designed pavements. GDOT has integrated their operational policies alongside the other data requirements of the calibration to ensure that all parameters represent the state's conditions. The following data was the result of their calibration for Flexible pavements.

<b>Model</b>	<b>Model Coefficients</b>	<b>Calibration Factor</b>
<b>IRI</b>	C1	2.2
	C2	2.2
	C4	6000
<b>Fatigue Cracking</b>	$\beta_{f1}$	0.00075
	$\beta_{f2}$	3.9491
	$\beta_{f3}$	1.2821
<b>Rutting</b>	$k_1$	-2.45
	$k_2$	0.30
	$k_3$	1.5606
	$\beta_{s1}$ for coarse grained soil	0.50
	$\beta_{s1}$ for fine grained soil	0.30

Table 2-5 Summary of local calibration factors for flexible pavements by Georgia DOT

A study was conducted by Timm to shed light on the local calibration of flexible pavement performance models. It reviewed the methodology undertaken by U.S. State highway agencies, the outcomes of their endeavor and the recommendations to implement the locally calibrated models. The study has found that calibration was performed based on reducing the error between measured and predicted values, by optimizing local calibration coefficients. Not all states agencies reported their method for sample size selection, while some even used a smaller than the minimum recommended amount by AASHTO. The results also varied from state agency to another. The rutting model produced the most bias and was more regularly over predicted, while the longitudinal cracking model was found

to have the poorest accuracy and hence the study recommends against using it. The summary Table 2-6 highlights the results of local calibration from different state agencies.

<b>Model</b>	<b>Verification</b>	<b>Calibration</b>	<b>Validation</b>
Fatigue Cracking	AZ, CO, IA, MO, NE States, NC, OR, UT, WA, WI	AZ, CO, NE States, NC, OR, WA	NA
Total Rutting	AZ, CO, IA, MO, NE States, NC, OH, OR, TN, UT, WA, WI	AZ, CO, IA, MO, NE States, NC, OH, OR, TN, UT, WA, WI	IA, NC
Transverse Cracking	AZ, CO, IA, MO, NE States, OH, OR, UT, WA, WI	AZ, CO, MO, OR, WI	
IRI	AZ, CO, IA, MO, NE States, OH, TN, UT, WA, WI	AZ, CO, MO, NE States, OH, WI	IA
Longitudinal Cracking	IA, NE States, OR, WA	IA, NE States, OR, WA	IA

*Table 2-6 Results of US States Local Calibrations*

In terms of Fatigue Cracking, all calibration efforts yielded better prediction results, with AZ and CO witnessing the most significant differences to the global model. As Table 2-6 shows, only four states eliminated or reduced bias, with NE states only reporting a reduction in the Sum of Squared Error with the calibration.

Furthermore, the transverse cracking calibration efforts resulted in improvements in Colorado and Missouri, producing reasonable results for the former, but with slight bias for the latter. The Arizona and Oregon attempts did not improve the prediction models and were hence their application was abandoned.

The longitudinal cracking calibration attempts resulted in an improvement in NE states, with a reported reduction in the SSE value after local calibration. In Iowa and Oregon, the SEE was large after calibration

For total rutting, improvements in the calibration results were witnessed in all participating states, with 8 out of 12 yielding improvements in the SEE and one resulting in an increase in SEE. Bias was reduced or eliminated in 8 of the states, with Ohio still experiencing bias, even after calibration. NE states, TN and WA did not report on bias but still experienced improvements in the prediction models.

All the investigated IRI calibration attempts showed improvements in IRI predictions with local calibration, with a reported increase in  $R^2$  value when compared to the default value of 56% (from global calibration). The NE states calculated the SSE and have indicated an improvement in the model. Missouri and Ohio have witnessed bias in the data but was deemed reasonable for the calibration effort.

## **Chapter 3: Data Collection and Methodology**

### **3.1 Hierarchical Input Levels**

The hierarchical approach to design inputs are adopted as it clearly defines the different levels of data input required in this research. It comprises of three data input levels and includes the attributes required for the MEPDG; design and materials, traffic and climate.

The parameters required for the first level of data input involve field and laboratory testing and data accumulation in the form of modulus testing, NDT testing and axle load data. These are resource hungry but are particularly important for specific site conditions as they provide high accuracy levels.

For the second level of input, access to agency or municipal database that include data from restricted testing, correlation examinations and/or regression analyses. The data can be in the form of predetermined dynamic modulus of binder, properties of the mix design constituents, traffic classification, volume and axle load. These are considered to have a medium level of accuracy.

The third level of data is usually user selected and is obtained from low traffic volume pavements that are not prone to early failure and are based on predefined values by the managing authorities. The data obtained from the input level is the least accurate from the three.

For the purpose of this research, Level 1 and 2 input parameters were utilized, indicating an intermediate level of accuracy. The data is mainly derived from MOID's database, which in the case of Level 2 Input's definition according to AASHTO (2008), is the local agency's database.

### **3.2 Data Collection Process**

Roads in the U.A.E are managed by three branches of Government. The main Governmental entity that oversees infrastructure development projects (mainly roads, bridges, dams) is the Ministry of Infrastructure Development, which is a department in the Federal Government. The second branch of Government are local municipalities, which are led by a local Government. In larger metropolitan cities like Abu Dhabi and Dubai, metropolitan Departments of Transport have been established (named Roads and Transport Authority in Dubai), and they share the authority over roads and bridges with the local municipalities.

The collection of data needed for this research started in October 2016, after contacting MOID in March of the same year. It took two years to obtain the data due to the unavailability of all the data required for the research. The Ministry has commissioned a Consultancy company to conduct condition surveys on its road network, this contract is ongoing. The 2017 data for IRI, Cracking and Rutting was collected while my request was open. This caused delays in starting the statistical analysis stage of the research, as data available did not suffice for the purpose of the research. Unfortunately, in the U.A.E, the establishment of a comprehensive pavement management system is a recent development. The oldest data available was from 2013. Moreover, condition surveys were not conducted on an annual basis and hence only two sets of data was available, for years 2013 and 2014. Other local municipalities were contacted but no response was received.

MOID has an ongoing consultancy contract with Rauros Group to improve their Pavement Management Practice, by deploying the latest technologies in pavement design

maintenance and management. The consultancy group utilizes the following tools to conduct pavement condition surveys, from which the researches data has been extracted.

- 1.LRMS = Laser Rut Measurement System
2. LCMS = Laser Crack Measurement System
3. Laser Profilometers = IRI Measurement
4. HRDMI = High Resolution Odometer for High accuracy chainage/Distance calculation

These tools are assembled in the vehicle shown in Figure 3-1.



*Figure 3-1 Condition Survey Equipment*

### **3.2.1 Data Components**

The process of assembling the essential data for calibration was done by two stages. In the first stage the available data provided by the Ministry of Infrastructure Development were evaluated to determine if the data can be used for the local Calibration. The required data is highlighted in figure 3-2 and is imperative to perform an ME Design. The

extensiveness of the data and accuracy will determine a better representation when carrying out the local calibration. The second stage ensured that the data in figure 3-2 was available for new flexible pavements built by the Ministry of Infrastructure Development.

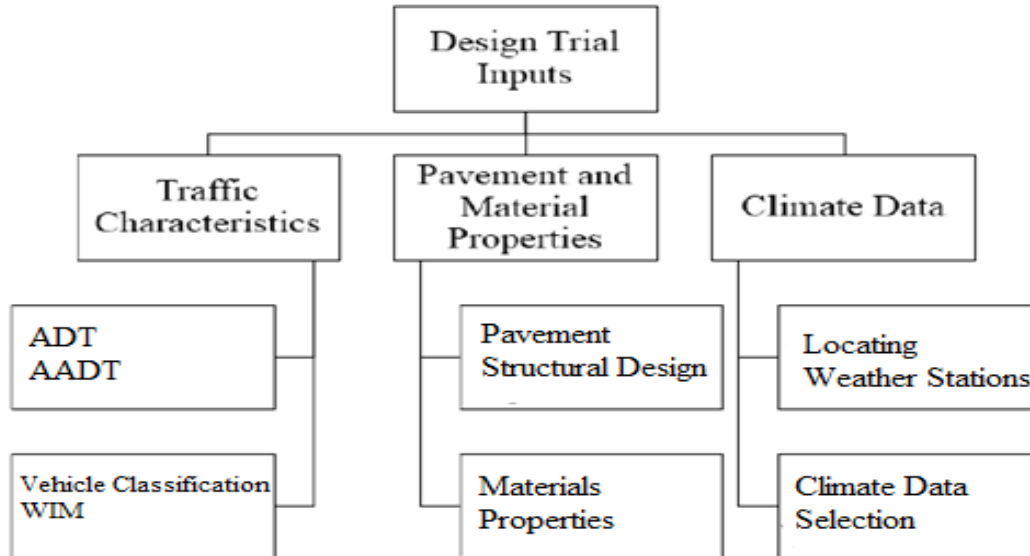


Figure 3-2 Data requirements for ME Design

The data was analyzed and the following data was acquired for each criteria:

- Climatic Data
  - Hourly weather and humidity data were collected from the National Center of Meteorology (NCM). The data spans from 1/1/2007 to 12/31/2008, covering a period of two years. The weather station chosen was that of Sharjah International Airport.
  - Only one station was needed since the climatic conditions are quite the same over the entire country, as the UAE covers a relatively small area.

Climate data collected as per ME Design software requirements has been recorded in Table 3-1.

- Traffic Data
  - Annual Average Daily traffic data has been obtained for the five main roads investigated.
  - Truck traffic volume: in the base year and the estimated growth rate in the design life was obtained.
  - Truck traffic volume adjustment factors, hourly and monthly, were not available and default software values were used
- Weigh in Motion Data
  - Axle load distribution factors: load spectra and vehicle class distribution were obtained
  - The U.A.E. has relatively lenient regulations in terms of weight of trucks utilizing a part of the road network. The maximum axle load of trucks was recorded as 20 metric tons, which is a very high figure by international standards.
  - AASHTOWARE ME 2.5.5 default values for general traffic inputs, such as axle configuration, wheelbase, and axles per truck will be used as the UAE adopts American standards

Traffic data collected as per ME Design software requirements has been recorded in Table 3-2.

- Structural Data and Materials Properties Data
  - 8 roadways with different structural design and configuration has been selected and tabulated in table 3-6.
  - Maps of the roadways have been obtained and are presented in figures 3-3



to 3-7.

- Obtained material properties of these roadways are available in appendix A and summaries of this data is presented in tables:
  - Table 3-3 Material properties inputs for Asphalt concrete
  - Table 3-4 Material properties inputs for Base, Subbase
  - Table 3-5 Materials properties for subgrade
- Where data was missing, default software values were used.
- Inbound and Outbound have been classified as follows:
  - Inbound E311 and E18-1 and E18-2: towards Ras Al Khaimah
  - Outbound E311 and E18-1 and E18-2: Away from Ras Al Khaimah
  - Inbound E99: Towards Kalba City in Sharjah
  - Outbound E99: Away from Kalba City towards Oman Border
- Distresses Data
  - IRI, Rutting and cracking data was obtained from MOID based on condition surveys from years 2013, 2014 and 2017.
  - MOID does not have set milepost measurements and hence to maintain uniformity of section lengths, distresses were averaged out for 0.5km sections.

The performance data is presented in appendix A

The Collected performance data from areas of similar conditions were used to compare and calibrate against pavement data received from the ministry. This approach is reasonable since areas of similar features and conditions have use similar pavement materials and structural configurations in the construction of flexible pavements.

Parameter	Input Parameter	Input Level	Value	Data Source
Climate	Temperature (C)	Level 1	Obtained	(c)
	Precipitation (mm)	Level 1	Obtained	(c)
	Windspeed (Kph)	Level 1	Obtained	(c)
	Sunshine (%)	Level 1	Obtained	(c)
	Humidity (%)	Level 1	Obtained	(c)
	Water Table (m)	Level 1	Obtained	(c)
	Location Coordinates	Level 1	Obtained	(c)

Table 3-1 Climate Parameters Inputs

Parameter	Input Parameter	Input Level	Value	Data Source
AADTT	Two-way AADTT	Level 2	3000	(a)
	Number of Lanes	Level 2	2,3,4	(a)
	Percent of Trucks in Design Direction	Level 2	12%	(b)
	Percent of Trucks in Design Lane	Level 2	60%	(b)
	Operational Speed	Level 2	80,100,140	(b)
Axle Configuration	Average Axle Width (m)	Level 2	Default	(d)
	Dual Tire Spacing (mm)	Level 2	Default	(d)
	Tire Pressure (kPa)	Level 2	Default	(d)
	Tandem axle spacing (m)	Level 2	Default	(d)
	Tridem axle spacing	Level 2	Default	(d)
	Quad axle spacing (m)	Level 2	Default	(d)
Lateral Traffic Wander	Mean wheel location (mm)	Level 2	Default	(d)
	Traffic wander standard deviation (mm)	Level 2	Default	(d)
	Design Lane Width	Level 2	Default	(d)
Wheelbase	Short Trucks – Average axle spacing (m)	Level 2	Default	(d)
	Medium Trucks – Average axle spacing (m)	Level 2	Default	(d)
	Long Trucks -Average axle spacing (m)	Level 2	Default	(d)
	Percent Short Trucks	Level 2	Default	(a)
	Percent Medium Trucks	Level 2	Default	(a)
	Percent Long Trucks	Level 2	Default	(a)
Traffic Volume Adjustment	Vehicle Class Distribution (Truck Traffic Classification - TTC)	Level 2	Calculated	(a)
	Traffic Growth Factor	Level 2	3%	(d)
	Monthly and Hourly adjustment	Level 2	Default	(a)
	Axles per truck	Level 2	Default	(d)
Axle Load Distribution	Axle Distribution (Single, Tandem, Tridem, Quad)	Level 2	Default	(a)

Table 3-2 Traffic parameters inputs

Parameter	Input Parameter	Input Level	Value	Data Source
<b>Asphalt Layer</b>	Thickness	Level 2	Obtained	(a)
<b>Mixture Volumetric</b>	Unit Weight (Kg/m <sup>3</sup> )	Level 2	2400	(d)
	Effective Binder Content by Volume (%)	Level 2	9.2	(a)
	Air Voids (%)	Level 2	6.0	(a)
<b>Poission's Ratio</b>		Level 2	0.35	(d)
<b>Mechanical Properties</b>	Dynamic Modulus	Level 2	Obtained	(a)
	G* Predictive Model	Level 2	Default	(d)
	Reference Temperature (C)	Level 2	Default	(d)
	Asphalt Binder	Level 2	Pen (60/70)	(a)
	Indirect Tensile Strength at 10C (MPa)	Level 2	Default	(d)
	Creep Compliance (1/GPa)	Level 2	Default	(d)
<b>Thermal Properties</b>	Thermal Conductivity (W/m-Kelvin)	Level 2	Default	(d)
	Heat Capacity (J/Kg-Kelvin)	Level 2	Default	(d)
	Thermal Contraction	Level 2	Default	(d)

Table 3-3 Asphalt concrete material properties inputs

Parameter	Input Parameter	Input Level	Value	Data Source
<b>Material</b>	Material Type	Level 2	Obtained	(a)
<b>Unbound Material Properties</b>	Thickness	Level 2	Obtained	(a)
	Poission's Ratio	Level 2	0.35	(d)
	Coefficient of Lateral Earth Pressure (K <sub>0</sub> )	Level 2	Default	(d)
<b>Modulus</b>	Resilient Modulus	Level 2	Obtained	(a)
<b>Sieve</b>	Aggregate Gradation	Level 2	Obtained	(a)
	Liquid Limit	Level 2	Obtained	(a)
	Plasticity Index	Level 2	Obtained	(a)
	Layer Compacted	Level 2	Obtained	(a)
	Maximum Dry Unit Weight (Kg/m <sup>3</sup> )	Level 2	Obtained	(a)
	Saturated Hydraulic Conductivity (m/hr)	Level 2	Default	(d)
	Specific Gravity of Solids	Level 2	Default	(d)
	Optimum Gravimetric Water Content (T)	Level 2	Default	(d)

Table 3-4 Base material properties inputs

Parameter	Input Parameter	Input Level	Value	Data Source
<b>Material</b>	Material Type	Level 2	Obtained	(a)
<b>Unbound Material Properties</b>	Thickness	Level 2	Obtained	(a)
	Poisson's Ratio	Level 2	0.35	(d)
	Coefficient of Lateral Earth Pressure (K <sub>o</sub> )	Level 2	Default	(d)
<b>Modulus</b>	Resilient Modulus	Level 2	Obtained	(a)
<b>Sieve</b>	Aggregate Gradation	Level 2	Obtained	(a)
	Liquid Limit	Level 2	Obtained	(a)
	Plasticity Index	Level 2	Obtained	(a)
	Layer Compacted	Level 2	Obtained	(a)
	Maximum Dry Unit Weight (Kg/m <sup>3</sup> )	Level 2	Obtained	(a)
	Saturated Hydraulic Conductivity (m/hr)	Level 2	Default	(d)
	Specific Gravity of Solids	Level 2	Default	(d)
	Optimum Gravimetric Water Content (T)	Level 2	Default	(d)

Table 3-5 Subgrade material properties inputs

Section	Road	Classification	Length (km)	Layer Thickness (cm)		
				Asphalt layers	Granular base	Granular Subbase
39,43,93,105	E311 OB	Freeway	70.950	12	15	45
25,47,115	E311 IB	Freeway	70.950	18	15	45
41,77	E18-2 OB	Primary Arterial	41.640	18	20	30
1,3,11	E18-1 IB	Primary Arterial	53.360	16	20	30
54,60	E18-1 OB	Primary Arterial	53.360	18	20	30
9,19	E99 OB	Primary Arterial	15.600	12	-	45
1,19,21,25	E99 IB	Primary Arterial	15.600	12	-	45

Table 3-6 Roadway classification and structural layer thicknesses

### **3.2.2 Selection of Pavement Sections**

When choosing the pavement sections that are used in this research, the materials used in the pavement design, the type of soil and the design of pavement layers was taken into account. Furthermore, traffic data, including Weigh In Motion Data, and the climate data is needed to conduct the local calibration and the MEPDG validation. Data from 3 condition surveys has been collected so that it would be possible to distinguish a pattern of distress evaluation when presented graphically in terms of mathematical charts. That have been carried out on relatively old pavement sections, of at least 10 years of operation. This will assist in producing accurate data that would provide strong relationships between design, use and performance. If a pavement has undergone some form of overlay, the history of distress, before and after the overlay will be very useful. Methods of calibration rely heavily on the data obtained. Hence there is a strong emphasis on the validity of the data. Heavily distressed pavements were the main source of data for this research. The research will focus on twenty pavement sections taken from different locations around the UAE. They are from regions that are, mountainous, sandy coastal or inland desert.

Four roadways have been selected from the road network displayed in the map above. Different classification of roads have been selected to have a more comprehensive study that would yield more accurate calibration factors. All the roads selected are flexible pavements constructed from the 1980s to 2008, in the three types of terrain that exist in the U.A.E; Desert, Coastal and Mountainous. The total length of the roads being researched is 409.5km. Maps of the roadways have been obtained and are presented in the following figures:

- Figure 3-3 shows a holistic map of the UAE's road network in the northern





Figure 3-5 Map of E311

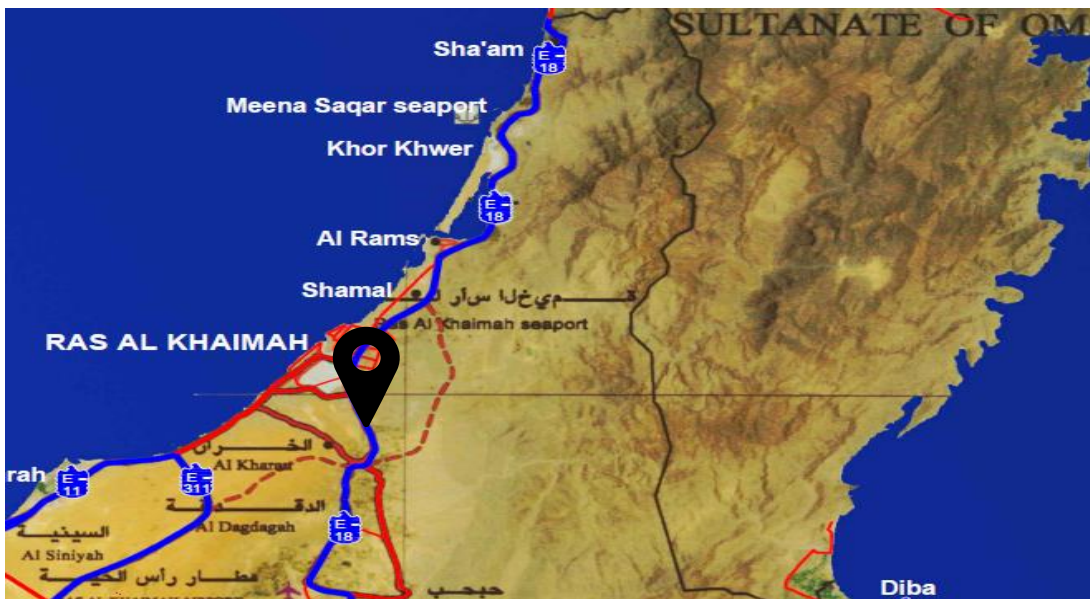


Figure 3-7 Map of E18-1



Figure 3-6 Map of E-99

### **3.3 Criteria for MEPDG Pavement Design**

The prediction models were run using the MEPDG for a collection of data including; flexible pavement layer material and design for current UAE roads, climatic data for the area examined and traffic data. The data was computed into the software using the following conditions:

- Design for a new flexible pavement structure.
- Design reliability of 50%, normally for calibration purposes.
- Construction date for each roadway.
- Pavement design structure for each roadway.
- Traffic data gathered from WIM station for vehicle classification and count
- Climate conditions from Sharjah International Airport weather station and NCMS website.
- Design life of 20 years in accordance with the design guide used by the U.A.E.

Since MEPDG runs were carried out for calibration purposes and the unavailability of all construction dates required in the software, a typical road construction schedule was adopted to compliment the given construction date for each roadway project. The unbound granular layer would be placed in late summer (September) where temperatures tend to cool down. The asphalt layer construction was considered to be a month later (October), while opening to traffic will take place in early winter (December). Seasonal attributes are reflective to local UAE conditions, where temperatures are relatively high most of the year with scarce precipitation all year round. These dates are reflected in the prediction distress values, where MEPDG accounts for the traffic loading of each month from the date of



opening the roads to traffic until the end of the computed design period (240 months).

Figure 3-6 presents the construction dates input tab for roadway E99.

Figure 3-8 E99 Construction Dates Input

To select the appropriate performance criteria values, MOID pavement threshold distress values that trigger rehabilitation with an overlay were obtained and computed into the software input tabs as shown in figure 3-9:

- Total rutting depth = 5.00mm
- Alligator cracking area in percent = 2%
- IRI = 2.00 m/km
- Reliability at 50% for calibration purposes

Performance Criteria	Limit	Reliability	Report Visibility
Initial IRI (m/km)	1		<input checked="" type="checkbox"/>
Terminal IRI (m/km)	2	50	<input checked="" type="checkbox"/>
AC top-down fatigue cracking (m/km)	100	50	<input checked="" type="checkbox"/>
AC bottom-up fatigue cracking (percent)	2	50	<input checked="" type="checkbox"/>
AC thermal cracking (m/km)	100	50	<input checked="" type="checkbox"/>
Permanent deformation - total pavement (mm)	5	50	<input checked="" type="checkbox"/>
Permanent deformation - AC only (mm)	2	50	<input checked="" type="checkbox"/>

Figure 3-9 Distress Threshold Criteria and Inputs

MOID provided the following performance:

1. IRI
  - a. IRI per lane

- b. Average IRI
- 2. Rut Depth
  - a. Rut per lane
  - b. Average Rut
- 3. Cracking
  - a. Block cracking per lane
  - b. Total Block cracking
  - c. Longitudinal cracking
  - d. Potholes per lane
  - e. Total potholes

To conduct a calibration of MEPDG, data for several distresses must be available. The data supplied by the Ministry does not include measurements of reflective or alligator cracks. Therefore, the calibration for cracking is not possible as the only usable cracking data will be that of Longitudinal cracking. Furthermore, a calibration of the IRI performance model will not be possible either due to the unavailability of alligator or transverse cracks; in the case of the rutting data, the total rutting data will have to be divided into the three rutting values, for each structural layer. The predicted rut depth values for each layer will be extracted from the MEPDG performance models to calculate the actual rut depth at each layer.

Rutting and Longitudinal cracking values are to be evaluated to investigate outliers and missing information will be carried out to ensure that the data sets used for calibration will produce accurate results. The average distress values for adjacent lanes will be the

used to conduct this analysis, while per lane values will not be used. Table 3-7 is a summary of the selected pavement sections and the measured distress values for each section.

No.	Project	Section	I. Chainage	F. Chainage	Condition Survey	Months after construction	Rutting	Longitudinal	IRI
1	E18-1-Inbound	1	0	500	10/01/2013	50	9.990	0.00	3.90
2	E18-1-Inbound	11	5000	5500	10/01/2013	50	10.705	0.00	3.72
3	E18-1-Outbound	54	26500	27000	10/01/2013	50	6.595	0.00	4.93
4	E18-1-Outbound	60	29500	30000	10/01/2013	50	6.860	0.00	4.44
5	E18-1-Inbound	3	1000	1500	10/01/2013	50	9.010	0.00	4.12
6	E99-Inbound	25	12000	12500	10/01/2013	170	5.600	0.00	2.08
7	E311-Inbound	25	12000	12500	10/01/2013	110	4.000	0.00	1.313
8	E99-Outbound	19	9000	9500	10/01/2013	170	6.875	0.00	1.93
9	E311-Outbound	39	19000	19500	10/01/2013	110	3.250	0.00	1.700
10	E311-Outbound	105	52000	52500	19/03/2014	124	4.770	0.00	1.257
11	E311-Inbound	115	57000	57500	19/03/2014	124	5.850	0.00	2.034
12	E311-Outbound	43	21000	21500	19/03/2014	124	6.850	0.00	2.518
13	E99-Outbound	9	4000	4500	07/04/2014	185	8.980	0.00	2.50
14	E18-2-Outbound	77	38000	38500	07/04/2014	72	4.450	0.00	2.30
15	E18-2-Outbound	41	20000	20500	07/04/2014	72	6.650	0.07	5.90
16	E311-Inbound	47	23000	23500	08/12/2017	168	6.265	0.00	1.66
17	E311-Outbound	93	46000	46500	08/12/2017	168	6.750	0.00	1.29
18	E99-Inbound	21	10000	10500	10/12/2017	228	7.270	0.00	2.40
19	E99-Inbound	19	9000	9500	10/12/2017	228	9.970	0.00	4.28
20	E99-Outbound	1	0	500	17/12/2017	228	9.480	0.00	1.90

Table 3-7 Measured Distress Values

Table 3-8 highlights the very low longitudinal cracking values. There is barely any sign of cracking on the pavement, when compared to the threshold value of 2m/km.

Statistical Values	Rutting (mm)	Longitudinal Cracking (m/km)	IRI (m/km)
Min	3.250	0.000	1.257
Max	10.705	0.070	5.900
Mean	7.009	0.004	2.808
Standard Deviation	2.108	0.016	1.366
Design Threshold	5.000	2.000	2.000

Table 3-8 Statistical Summary for Distress Values of Investigated Sections

The initial statistical analysis for the selected sections indicates that rutting is significant exhibiting a mean higher than the design threshold, with a standard deviation of

2.108. This shows that rutting is an issue that needs to be investigated. In contrast, longitudinal cracking is very insignificant with a maximum distress value of 0.07m/km, a mean of 0.04 and standard deviation of 0.016. This reflects the unsuitability of this distress to perform a local calibration. It also shows, as already known by practitioners that cracking is rarely present on the UAE pavements that are exposed to high temperatures: rutting is the major concern. Cracking is rarely observed also because asphalt mixes in the UAE tend to have a higher bitumen content than mixes used in the U.S.A. Higher bitumen content makes mixes more ductile and therefore, less susceptible to cracking. Finally, IRI values gave a mean value of 2.808m/km and a standard deviation of 1.366 m/km was recorded.

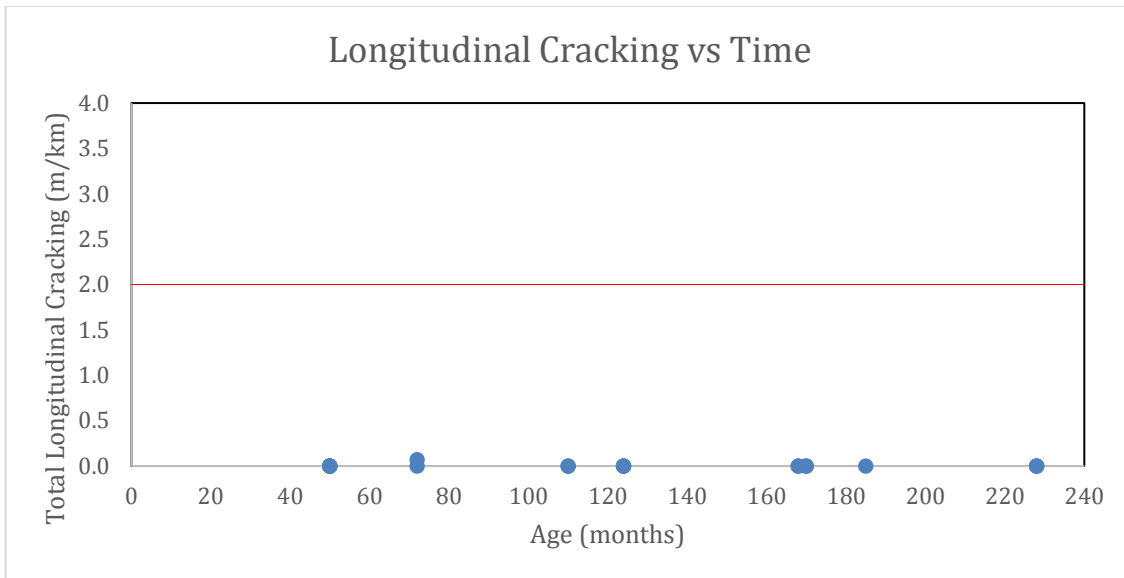


Figure 3-10 Longitudinal Cracking vs. Time Plot

The longitudinal Cracking over Time plot shown in Figure 3-10 clearly shows that cracking is nearly non-existent in the investigated sections. This indicates that the data cannot be used to perform a local calibration as data is clearly tilted towards the lower end, with weak dispersion of data points.

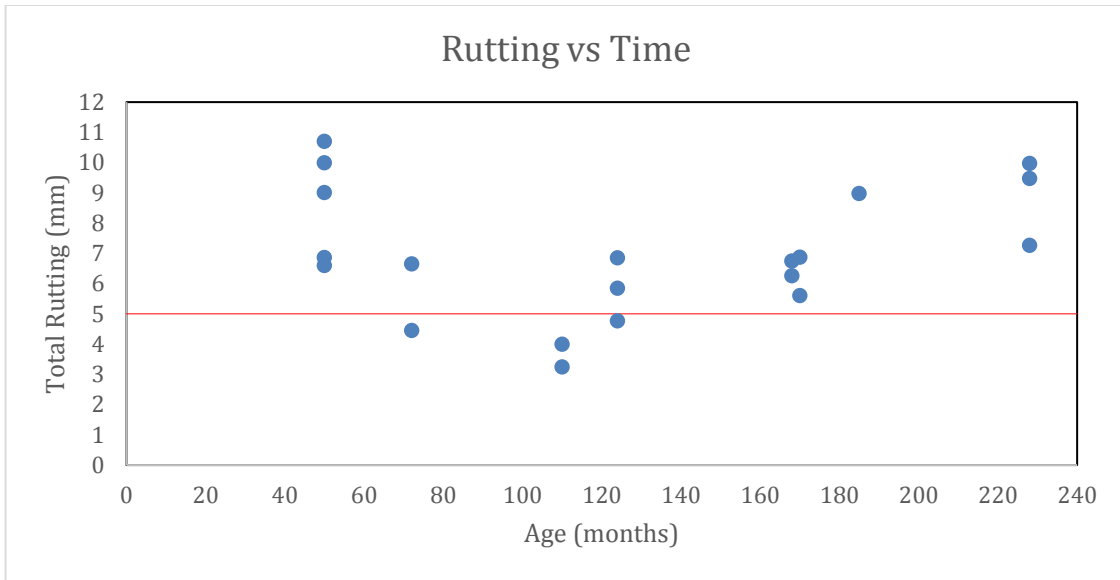


Figure 3-11 Rutting vs. Time Plot

Figure 3-11 indicate that the available data is reasonable with significant rut depths exceeding the threshold value set by MOID. The data points exhibit a good dispersion which makes rutting useful for local calibration.

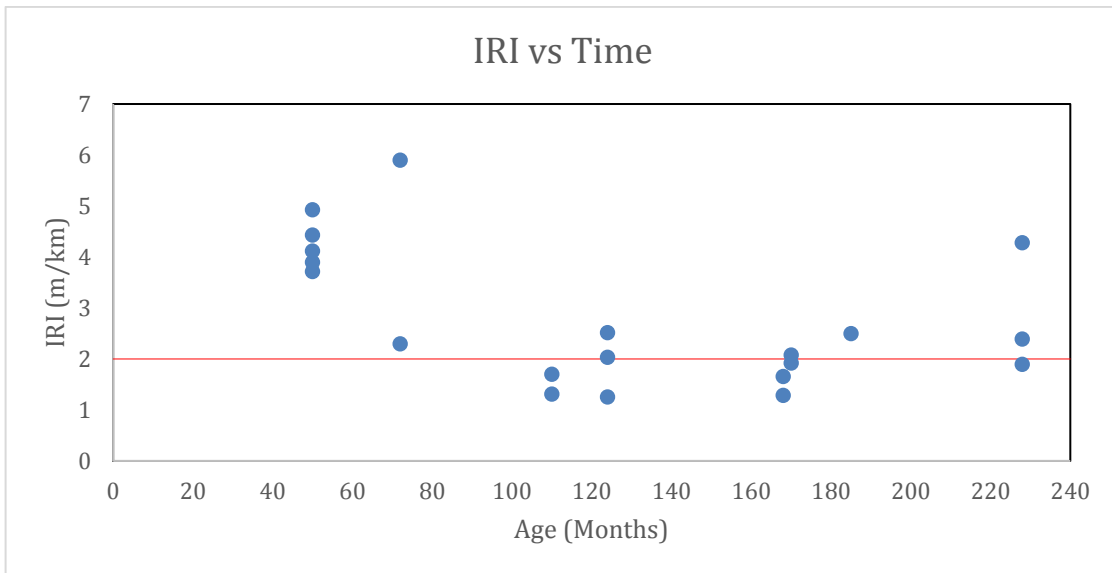


Figure 3-12 IRI vs. Time Plot

Figure 3-12 indicate that the available IRI data is reasonable but not as significant as the rut depths. Most of the data points are within the threshold value. The age aspect of

the plot indicates that IRI was more severe at 50 months values but are within the critical values later. This may show a resurfacing procedure may have been carried out. Generally, the data points exhibit a good dispersion which will may be useful for local calibration. Values of 0 will be used for the fatigue and transverse cracking coefficients to perform a local calibration for IRI.

### **3.4 Pavement Materials Data**

The Ministry of Infrastructure Development (MOID) typically constructs a full depth asphalt pavement using the AASHTO 1993 empirical design method. The structure of the flexible pavement comprises of a surface asphalt layer, an unbound base layer and a subgrade layer. In fine grain soil situations, the subgrade is stabilized while in coarse grain soils, mainly in mountainous regions, the subgrade may needn't be stabilized. The material properties of each layer were supplied by MOID with the extensiveness available. In instances where information was missing, the software supplied specifications were used as the UAE generally uses American Standards in pavement construction.

The pavements investigated have different thicknesses for all the structural layers and hence the MEPDG software was run 8 times to get performance predictions for every roadway being investigated. The resilient modulus was adjusted according to the supplied data to accommodate local conditions. Subchapters 3.4.1 covers the asphalt layer structural thickness and property and subchapter 3.4.2 covers the unbound granular layer (for base and subgrade) inputs applied to the software.

### 3.4.1 Asphalt Concrete Volumetric Properties

Both MOID data and software default values were used to assemble the volumetric properties since, in some cases, certain specifications were not provided by the local agency.

- For Air Void content, a value of 6% was recommended by the Ministry, while the effective binder content was computed as 9.2% by volume.
- For Poisson's ratio, the default value of 0.35 was used.
- As recommended and used by MOID a bitumen grade classified as Conventional Penetration Pen (60-70) is used for the Asphalt Binder in all their Pavement Designs.
- MOID has specified an aggregate gradation for the Asphalt mix which was inputted in the MEPDG software input tab. Four different Asphalt Layer design documents were provided by the Ministry, covering different road classifications constructed by them. The gradation selected is that used for Freeways and Primary Arterials, which corresponds to the road sections analyzed in this research. These roads have significant distress, mainly due to increasing traffic loads.

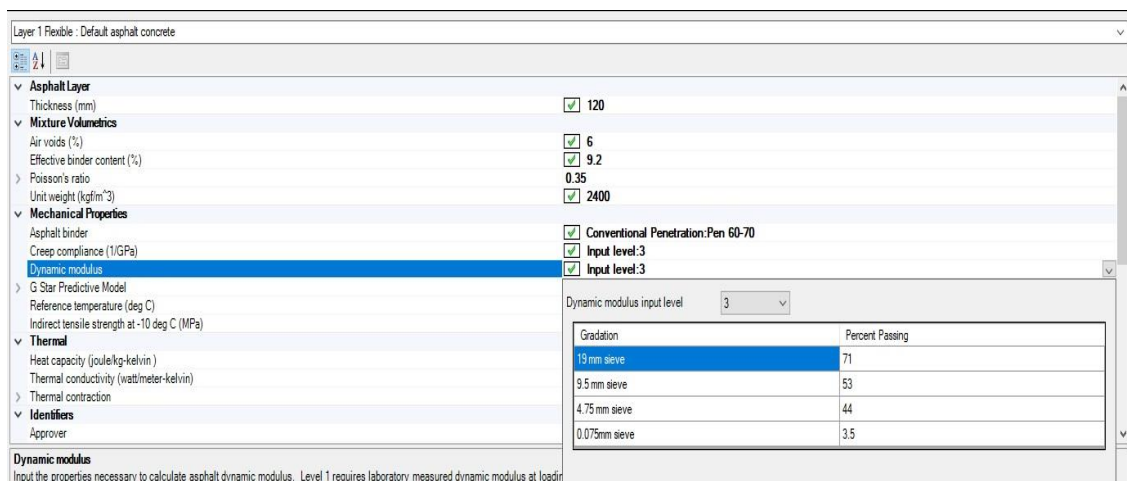


Figure 3-13 Asphalt layer inputs

- Default values were used for Creep Compliance, Reference Temperature and Indirect tensile strength and Thermal values as they were not provided by MOID and they are rarely measured.

### **3.4.2 Unbound Layer Properties**

Base and Subbase Properties Consists of hard durable natural or crushed stones free from clay and other deleterious material

- CBR @ 95% Compaction- >60%
- Liquid Limit – Max 35
- Plasticity Index - <6
- Maximum Dry Density – Min.2.10 Mg/M<sup>3</sup>
- Aggregate Soundness (MgSo4) – Max 12%
- Linear Shrinkage - Max 3%
- Chloride Content – Max 1%
- Sulphate Content – Max 0.5%

<b>BS SIEVE</b>	<b>% PASSING</b>
50mm	100
25mm	80-100
12.5mm	60-85
4.75mm	40-70
2.00mm	20-50
850 microns	15-25
425 microns	0-10
180 microns	0-2

*Table 3-9 Base, Subbase gradation information was provided by MOID*

Level 2 design input was selected to an adjustment of the resilient modulus based on the design specifications provided by MOID as shown in Table 3-9 above. Moreover, MOID and ADM specification were used to determine the unbound materials design



inputs. The local agencies provided general aggregate gradation tables, which were used in the data input phase as shown in Figure 3-14 below.

Layer 2 Non-stabilized Base : A-3 (A-1-a)	
<input checked="" type="checkbox"/> <b>Unbound</b>	
Coefficient of lateral earth pressure (k0)	<input checked="" type="checkbox"/> 0.5
Layer thickness (mm)	<input checked="" type="checkbox"/> 200
Poisson's ratio	<input checked="" type="checkbox"/> 0.35
<input checked="" type="checkbox"/> <b>Modulus</b>	
Resilient modulus (MPa)	<input checked="" type="checkbox"/> 110
<input checked="" type="checkbox"/> <b>Sieve</b>	
Gradation & other engineering properties	<input checked="" type="checkbox"/> A-1-a
<input checked="" type="checkbox"/> <b>Identifiers</b>	
Approver	
Date approved	1/1/2011
Author	AASHTO
Date created	1/1/2011
County	
Description of object	Default material
Direction of travel	
Display name/identifier	A-3
District	
From station (km)	
Item Locked?	False

Figure 3-14 Non Stabilized Base Input

According to the adjustment to the gradation inputs, AASHTO classifies the unbound base layer as type A-1-a.

### **3.4.3 Subgrade Layer Properties**

MOID recommends the following specification for the subgrade used in the pavement design

- a. Dune Sand
  - CBR @ 95% Compaction- < 15,
  - Plasticity Index -Non plastic
  - Maximum Dry Density – Around 1.69 to 1.75 Mg/M<sup>3</sup>
- b. Gravel Material
  - CBR @ 95% Compaction- >40
  - Plasticity Index - <6
  - Maximum Dry Density – 1.90 to 2.30 Mg/M<sup>3</sup>

- Compacted with optimum moisture to 98% of MDD

The AASHTOWARE software recommended an unbound layer type A-1-a as per the software inputs. The gradation has been adjusted to concur with local specifications provided by the Ministry. Figure 3-15 highlights the software inputs for the recommended design.

Sieve Size	Percent Passing
0.001mm	
0.002mm	
0.020mm	
0.075mm	5
0.150mm	
0.180mm	
0.250mm	
0.300mm	
0.425mm	
0.600mm	
0.850mm	
1.18mm	
2.0mm	22
2.36mm	
4.75mm	34
9.5mm	44
12.5mm	51
19.0mm	61
25.0mm	
37.5mm	99
50.0mm	100
63.0mm	
75.0mm	
90.0mm	

Liquid Limit	11
Plasticity Index	0
<input checked="" type="checkbox"/> Is layer compacted?	
<input checked="" type="checkbox"/> Maximum dry unit weight (kgf/m <sup>3</sup> )	1922.2
<input type="checkbox"/> Saturated hydraulic conductivity (m/hr)	2.209e-01
<input type="checkbox"/> Specific gravity of solids	2.7
<input type="checkbox"/> Water Content (%)	10.2
<input type="checkbox"/> User-defined Soil Water Characteristic Curve (SWCC)	

af	1.30574690972311
bf	2.42732220482246
cf	0.746646511250896
hr	100

Figure 3-15 Subgrade Gradation and properties Input

### **3.5 Traffic Data**

The MEPDG requires several traffic inputs to perform the design process. All of these traffic inputs were obtained from MOID and can be considered as Level 1 design inputs. In addition, the rest of traffic inputs were used as Level 3 inputs or based on the MOID and ADM requirements. These traffic inputs are:

- Annual Average Daily Truck Traffic (AADTT): AADTT values assumed as 3000.
- Number of Lanes in Design Direction: 2 lanes

- Percentage of Trucks in Design Direction: 12%
- Percentage of Trucks in Design Lane: 60%
- Operational Speed: Varies from 80, 120 and 140km/h
- Truck Traffic Growth Rate: The exponential traffic growth model, with a growth rate of 3% was used. This is the value recommended by MOID.

E-99-Inbound:Project*		E-99-Inbound:Climate		E-99-Inbound:Traffic	
<b>▼ AADTT</b>					
Two-way AADTT	<input checked="" type="checkbox"/>	3000			
Number of lanes	<input checked="" type="checkbox"/>	2			
Percent trucks in design direction	<input checked="" type="checkbox"/>	12			
Percent trucks in design lane	<input checked="" type="checkbox"/>	60			
Operational speed (kph)	<input checked="" type="checkbox"/>	80			
<b>▼ Traffic Capacity</b>					
Traffic Capacity Cap	<input checked="" type="checkbox"/>	Not enforced			
<b>▼ Axle Configuration</b>					
Average axle width (m)	<input checked="" type="checkbox"/>	2.59			
Tandem axle spacing (m)	<input checked="" type="checkbox"/>	1.31			
Dual tire spacing (mm)	<input checked="" type="checkbox"/>	305			
Quad axle spacing (m)	<input checked="" type="checkbox"/>	1.25			
Tire pressure (kPa)	<input checked="" type="checkbox"/>	827.4			
Tridem axle spacing (m)	<input checked="" type="checkbox"/>	1.25			
<b>▼ Lateral Wander</b>					
Design lane width (m)	<input checked="" type="checkbox"/>	3.7			
Mean wheel location (mm)	<input checked="" type="checkbox"/>	460			
Traffic wander standard deviation (mm)	<input checked="" type="checkbox"/>	254			
<b>▼ Wheelbase</b>					
Average spacing of long axles (m)	<input checked="" type="checkbox"/>	5.49			
Average spacing of medium axles (m)	<input checked="" type="checkbox"/>	4.57			
Percent trucks with long axles	<input checked="" type="checkbox"/>	61			
Percent trucks with medium axles	<input checked="" type="checkbox"/>	22			
Percent trucks with short axles	<input checked="" type="checkbox"/>	17			
Average spacing of short axles (m)	<input checked="" type="checkbox"/>	3.66			

Figure 3-16 Traffic Inputs

The default values were used for the other general traffic inputs are:

- Number of Axels/Truck
- Axle Configuration
- Lateral Wander
- Wheel base

Data from one Weigh In Motion (WIM) station was provided by MOID. The data has counts for vehicle classes; 4, 5, 6, 8, 9 and 10, with lower classes considered as light vehicles. Vehicles of higher class (11-13) are not used in the UAE. Class 7 vehicles are not used in the UAE as well. Figure 3-17 shows the different vehicle axle types as classified by the Federal Highways Agency (FHWA) and is adopted by MOID.








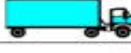









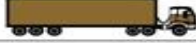
















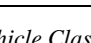

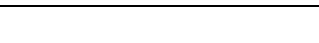


<b>Class 1</b> Motorcycles		<b>Class 7</b> Four or more axle, single unit	
<b>Class 2</b> Passenger cars		<b>Class 8</b> Four or less axle, single trailer	
			
			
			
<b>Class 3</b> Four tire, single unit		<b>Class 9</b> 5-Axle tractor semitrailer	
			
			
<b>Class 4</b> Buses		<b>Class 10</b> Six or more axle, single trailer	
			
			
<b>Class 5</b> Two axle, six tire, single unit		<b>Class 11</b> Five or less axle, multi trailer	
			
			
<b>Class 6</b> Three axle, single unit		<b>Class 12</b> Six axle, multi-trailer	
			
			
			
		<b>Class 13</b> Seven or more axle, multi-trailer	
			
			

Figure 3-17 FHWA Vehicle Classification

Figure 3-18 shows the vehicle distribution inputs which were calculated from WIM station counts for vehicle classes 4,5,6,8,9 and 10. The growth rate is set at 3%.

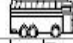
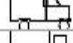
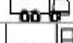

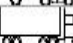

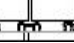

Vehicle Class Distribution and Growth				Load Default Distribution
Vehicle Class	Distribution (%)	Growth Rate (%)	Growth Function	
Class 4	0.94	3	Linear	
Class 5	5.14	3	Linear	
Class 6	2.87	3	Linear	
Class 7	0	3	Linear	
Class 8	33.32	3	Linear	
Class 9	9.64	3	Linear	
Class 10	48.09	3	Linear	
Class 11	0	3	Linear	

Figure 3-18 Vehicle Classification Distribution and Growth Input

### **3.6 Climate Data Assembling**

Climate information is essential for the mechanistic iteration in the performance models using in MEPDG. It quantifies the effects of temperature and moisture on stiffness at each of the pavement's structural layers. These are also used in the smoothness prediction model to calculate the site factor. AASHTOWARE software uses climate data files from Modern Era Retrospective-Analysis for Research and Applications (MERRA) to perform the pavement design process. The MERRA database provides data from climate stations throughout the United States and Canada. The data categories cover: hourly climate data for; temperature, humidity, precipitation, windspeed and sunlight (MAUPIN, 2006). It also provides the measurement of water-table for the selected weather station. Figure 3-19 shows a map of the weather stations available in the selected area. A weather station is chosen to compute the climatic data of that station in the software.

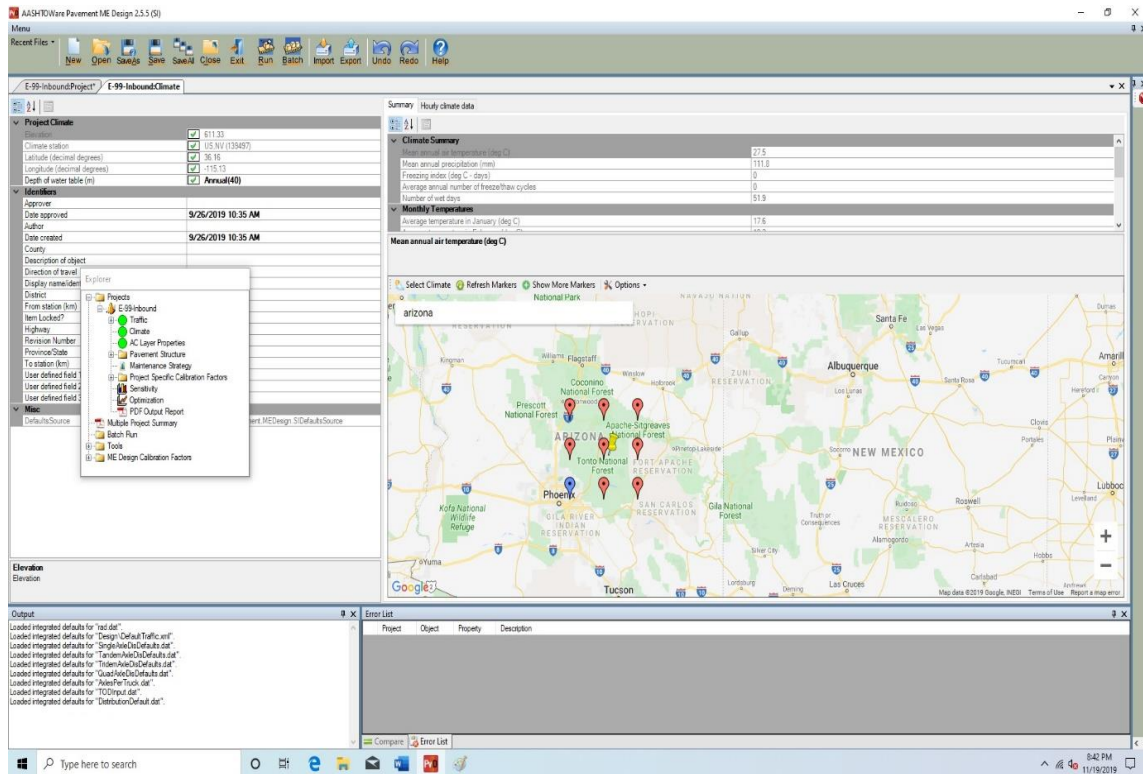


Figure 3-19 Climate Data Selection

Unfortunately, the software doesn't have access to global weather stations. To overcome this issue, the National Center of Meteorology (NCMS) in the UAE was approached to acquire the climate data sets required. NCMS supplied hourly temperature, and humidity for two years, as it is the least requirement to use the AASHTO Pavement ME Design software. The data was obtained for the period from 1/1/2017 to 12/31/2018. For the remaining data; precipitation, sunlight and windspeed, monthly averages were obtained from the NCMS website. The monthly averages was expanded to cover hourly information. Average measurements of water table were obtained for the roadway projects selected.

The climate data from U.S. weather stations are stored in files with .hcd extension. Hence to transfer the obtained information to the software, a random weather station was selected in the U.S. and the climate data file was downloaded and imported to AASHTOWare. The existing climate data in the file downloaded was then replaced with the two-year data acquired from NCMS in the UAE. Only one weather station was used due to the assumption that only minor variation in climate exists between the roadways being investigated. Figure 3-20 shows how the data from the weather station is set into the software.

Summary Hourly climate data						
January /2007		to		December/2008		Verify Weather
Date/Hour	Temperature (deg C)	Wind Speed (kph)	Sunshine (%)	Precipitation (mm)	Humidity (%)	Water table (m)
1/1/2007 12:00:00 AM	16.6	10.8	0	0	58	40
1/1/2007 1:00:00 AM	17	10.8	0	0	58	40
1/1/2007 2:00:00 AM	16.6	10.8	0	0	58	40
1/1/2007 3:00:00 AM	16.2	10.8	0	1	61	40
1/1/2007 4:00:00 AM	15.7	10.8	0	0	62	40
1/1/2007 5:00:00 AM	15.6	10.8	0	0	63	40
1/1/2007 6:00:00 AM	15	10.8	0	0	66	40
1/1/2007 7:00:00 AM	14.6	10.8	0	0	70	40
1/1/2007 8:00:00 AM	14.7	10.8	100	0	70	40
1/1/2007 9:00:00 AM	16.3	10.8	100	0	64	40
1/1/2007 10:00:00 AM	18.1	10.8	100	0	55	40
1/1/2007 11:00:00 AM	19	10.8	100	0	51	40
1/1/2007 12:00:00 PM	19.7	10.8	100	0	49	40
1/1/2007 1:00:00 PM	20.1	10.8	100	0	49	40
1/1/2007 2:00:00 PM	20.4	10.8	100	0	47	40
1/1/2007 3:00:00 PM	19.8	10.8	100	0	50	40
1/1/2007 4:00:00 PM	20	10.8	100	0	50	40
1/1/2007 5:00:00 PM	19.2	10.8	100	0	52	40

Figure 3-20 Climate Data Computations

## **Chapter 4: Local Calibration and Validation Plan**

The chapter explains the plan for the local calibration and validation of MEPDG for conditions of the UAE. This plan is laid out in the instructions' guidebook published by AASHTO, namely the Guide for the Local Calibration of the Mechanistic-Empirical Pavement Design Guide (AASHTO, 2010).

Pavement distress prediction models are utilized in Mechanistic Empirical analysis. These must be validated against measured distress from in-situ pavement structures in order to conduct the calibration process for local conditions. The calibration process is then validated statistically using the available measured data to improve the accuracy of the prediction models. An acceptable correlation between the examined sets of data is imperative to produce confident calibration coefficients. A regression analysis is conducted with the selected set of sections examined (the number of sections depends on the distress being analyzed), to yield the calibration coefficient. In this way, the transfer functions or distress models are calibrated to the local conditions of the roads investigated.

A calibration is a statistical approach to reduce the total error between the predicted and measured values by calculating the residuals and then optimizing the model to yield the lowest possible sum of squared error (SSE). The model is thus validated to ensure that the calibration model will yield more accurate results even when computing different data from similar sets. This gives the developed model a sense of legitimacy, allowing for reliable future predictions. Bias testing and elimination procedures are utilized in the calibration model to ensure the reliability of the transfer functions yielded through the calibration process.



#### **4.1 Developing the Performance Models for Ministry of Infrastructure Development**

It is imperative to calibrate performance models to accommodate local conditions as default MEPDG performance models are based on calibration performed using Long Term Pavement Performance (LTPP) database, which contains pavement performance data for test sections in the United States and Canada. Therefore, the model calibration is required to reduce the errors between the predicted values and the actual values. This difference is caused due to a change in climate, traffic characteristics, and design specifications.

Local calibration will be performed for total rutting and roughness, measured by the International Roughness Index (IRI). The estimation of local bias will determine the reliability of the data, and whether to adopt in the research or to be abandoned.

- Selection of Number of Pavement Sections
- Threshold values indicated by the MOID at
  - Total Rutting = 5mm
  - IRI = 2m/km
- Standard Error of Estimate for rutting and IRI will be calculated based on recommendations from MEPDG
- Confidence Level to be selected would be at 95%.
- Calculate Mean and Standard Deviation of Distresses
- Construct Scatter Plots of Predicted and Measured Distresses

#### **4.2 Local Bias Assessment**

- Run data in MEPDG software using global parameters to produced

predicted data.

- Compare Actual vs. Predicted Values to determine:
  1. Bias
  2. Standard Error of Estimate
  3. Residuals
- Determine p-value for the slope
- Local Bias assessed by studying the null hypothesis that average residual error is 0 at 95% confidence level
- Reject if p-value < 0.05
- Plot scatter charts of Actual vs Predicted data to determine the dispersion around the line of equality.

The bias elimination process is used when a significant level of bias is witnessed from the preliminary statistical analysis of the predicted values against the measured values as shown in Figure 4-1. It depends on the possible causes of the bias and the required accuracy by the local agency.

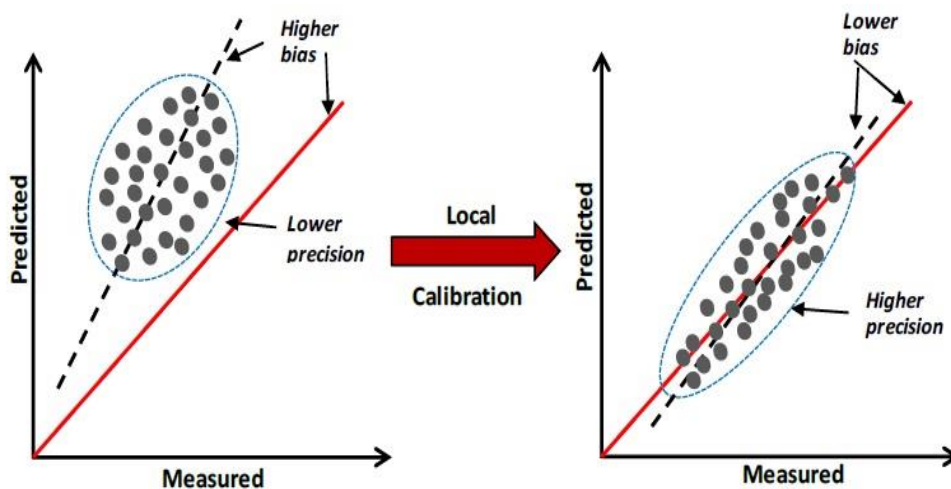


Figure 4-1 Improvement in Bias and Precision

There are three main reasons that could lead to a certain degree of bias.

1. The residual errors are polarized, either negative or positive, for the most part and the Plots of residual errors against predicted values is generally constant and near the zero value. This indicates that the global performance model is adequate but with poor accuracy, demonstrating a strong bias. This requires a local calibration to reduce the bias, with a limited number of iterations required.
2. There is a low bias and the values are quite constant with time, but with large dispersions in residual values, with positive and negative values. In this case, the performance model equation is used to adapt the coefficient factors, but some underlying issues included in the data sets influence the data. This situation may require more software runs to reduce the bias.
3. The residual errors vs predicted values plot shows a strong dependence on the predicted values. This indicates that the performance model is poor and not marginally reflective of the measured values, reflected in a poor correlation between the measured and the predicted values. This situation requires most iterations due to the complexity of loading cycles (times) component, which needs to be considered.

#### **4.3 Conduct local calibration to determine transfer functions**

Applied Simple Linear Regression will be used to determine correlation between actual distress and predicted distress

- Predicted distress assigned as independent variable (x)
- Measured distress assigned as dependent variable (y)
- The Regression Analysis would determine the calibration factors

#### **4.4 Performance Models Validation**

A Goodness of Fit testing validation approach will be performed for the performance data analyzed by the Ministry (rutting and IRI models). This analytical procedure will refine and confirm the calibration coefficients for the distress prediction models. It utilizes goodness of fit statistics that measures the standard error of estimate and compares the values against global criteria, which results in more accurate prediction models.

## Chapter 5: Development of Local Calibration Models

This chapter will describe the process to develop a local calibration of the MEPDG performance models to the UAE’s local conditions. Initially, the research will investigate the significance of bias of the predicted distresses. This will be assessed using a hypothesis testing, by determining the p-value from the computation of both the actual and predicted data. The other assessment will be to determine a Goodness of fit test as a method of validation for the regression of the actual and predicted data. This will be assessed by calculating the Standard Error of Estimate and comparing it with threshold values, selected based on the desired accuracy of each distress prediction. The criteria that will be used to determine the soundness of the analysis and results are laid out in Table 5-1.

<b>Criteria</b>	<b>Test</b>	<b>Threshold</b>
<b>Bias</b>	Hypothesis test of intercept (predicted x vs actual y)	p-value Reject hypothesis if p-value is <0.05
<b>Goodness of Fit</b>	SEE for Rutting	0.1in or 2.54 mm
	SEE for IRI	17in/mi or 0.268 m/km

*Table 5-1 Criteria for Adequacy of Global Model*

### **5.1 Assess Local Bias for Global Calibration**

The MEPDG performance models used in AASHTOWARE 2.5.5 yielded predicted results using the Global Calibration coefficients for each distress type for a reliability of 50%. The software produced files of predicted distress values for each distress type, at monthly intervals, covering the design life selected. This has produced values for 240 months. The predicted results were compared to the measured results for the selected pavement sections. Table 5-2 shows the months in which the condition survey was conducted per project. The predicted values were selected based on:

1. The pavement construction date
2. The date of the latest condition survey

Project	Date of Opening to Traffic	Last Survey Date	No. of Month Since Opening
E18-1 and E18-2	01/12/2008	10/01/2013	50
E311	01/12/2003	10/01/2013	110
E99	01/12/1998	10/01/2013	170
E18-1 and E18-2	01/12/2008	15/12/2014	72
E311	01/12/2003	19/03/2014	124
E99	01/12/1998	07/04/2014	185
E18-1 and E18-2	01/12/2008	17/12/2017	108
E311	01/12/2003	08/12/2017	168
E99	01/12/1998	10/12/2017	228

Table 5-2 Condition Survey Date in Months

Hence, 20 values were extracted for each distress type and were compared to the corresponding measured data. The comparison was carried out by calculating:

1. The mean error, from the residuals.
2. The sum of squared error (SSE).
3. The standard error of estimate (SEE).

A linear regression analysis between the predicted distress values (x) and the measured distress values (y) was conducted. The regression analysis produced the p-value which is used to test the null hypothesis to determine if there is a systematic difference between both the predicted and the measured values of distress. The hypothesis states that the mean error should be zero at a 95% confidence level as shown in the Equation 27:

$$H_0 = \sum_{i=1}^n (y_{measured} - x_{predicted}) = 0$$

Equation (27)

Where:

$y_{measured}$  = Measured distress values.

$x_{\text{predicted}}$  = predicted distress values based on global calibration.

In order to conduct comprehensive model analysis, the slope estimators should be used by carrying out a fitted regression model. The variability of the measured will also be plotted against the distributed errors of the predicted values. The regression model takes the following form:

$$\hat{y}_i = m(x_i)$$

Equation (28)

Where:

$\hat{y}_i$  is the estimator of mean measured values

$m$  is the slope

The slope values are used as the coefficient values, which will be the transfer functions to calibrate the performance models to accommodate local conditions. Table 5-3 summarizes the global regression coefficients used in the regression analysis, the mean error and the bias hypothesis based on the calculated p-value.

<b>Distress Type</b>	<b>Global Coefficient</b>	<b>Mean Error (<math>e_r</math>)</b>	<b>p-value</b>	<b>Hypothesis</b>
<b>Rutting</b>	$\beta_{1r} = 1$ $\beta_{s1} = 1$ $\beta_{s1} = 1$	-1.118	0.0636	Null hypothesis is not rejected $p > 0.05$
<b>IRI</b>	$C_1 = 40.0$ $C_2 = 0.4$ $C_3 = 0.008$ $C_4 = 0.015$	-1.49	0.0187	Null hypothesis is not rejected $p > 0.05$

Table 5-3 Bias Statistical Analysis Using Global Calibration

The p-value for the regression output from the rutting values yielded a value of:

$$0.0636 > 0.05$$

This indicates that the null hypothesis cannot be rejected and hence it cannot be concluded that the performance models produced biased prediction values.

The p-value for the regression output from IRI values yielded a value of:

$$0.0187 > 0.05$$

This indicates that the null hypothesis is rejected and hence the IRI model produces bias.

In terms of the data variability plot for rutting, exhibited in Figure 5-1, there is a uniform dispersion around the equality line with the majority of the data points above the equality line, indicating an under prediction of the distress value by the software's performance models. This is computed in the mean error calculation, with a mean error of -1.118 mm.

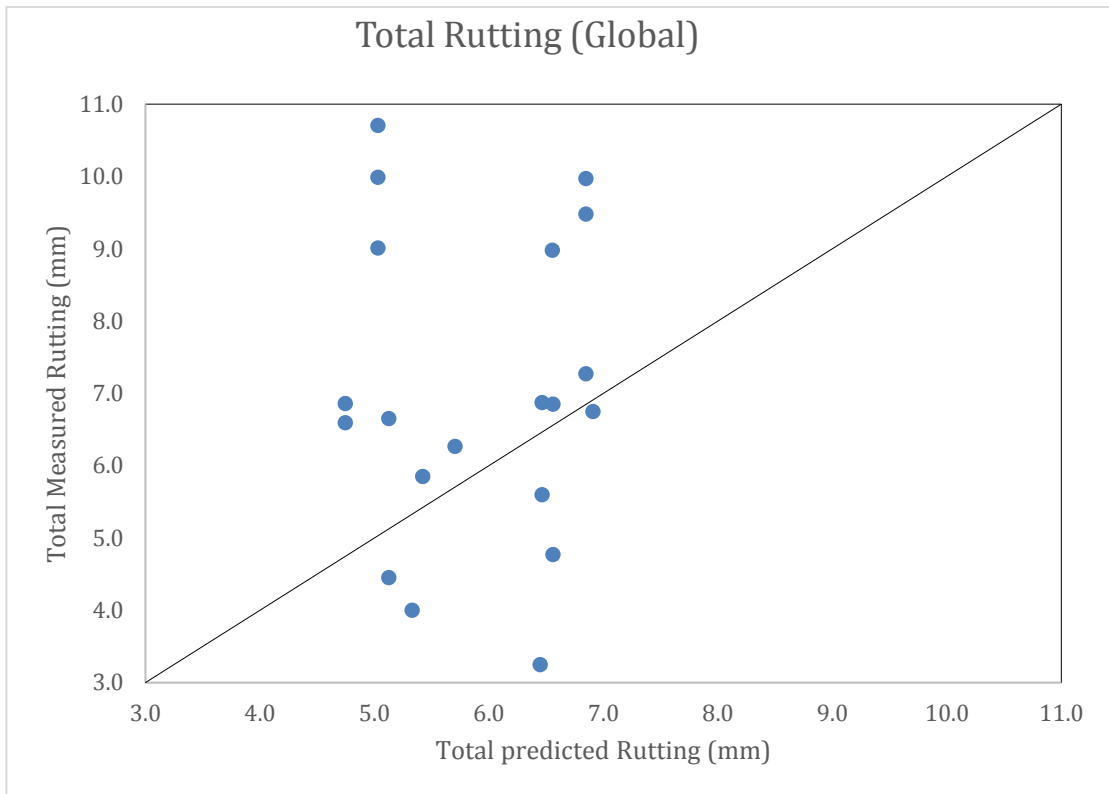


Figure 5-1 Total Measured Rutting vs Total predicted Rutting in Global Calibration

This requires an adjustment of the global calibration to produce a more uniform dispersion around the equality line. This will yield a local calibration of the performance models utilized by MEPDG.



In terms of the data variability plot for IRI, exhibited in Figure 5-2, there is a clear bias in the data with majority of the points above the equality line. This indicates an under prediction of the IRI values by the models. This is computed in the mean error calculation, with a mean error of -0.49 m/km.

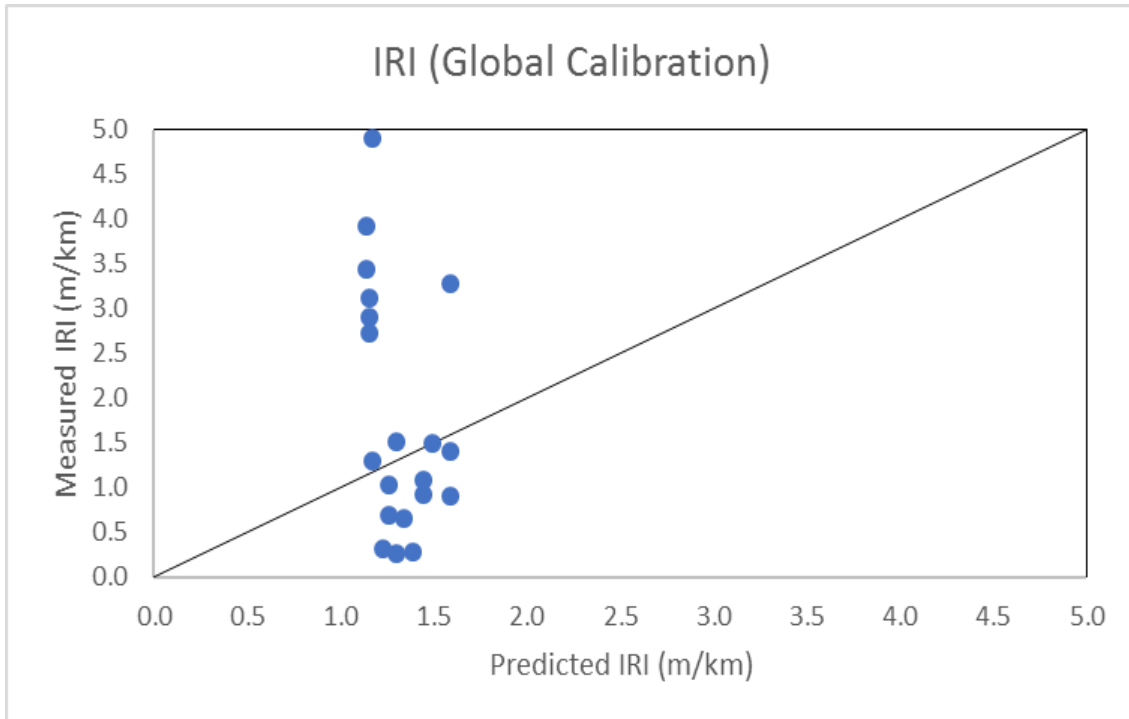


Figure 5-2 Measured IRI vs Predicted IRI based on Global Calibration

## **5.2 Eliminate Local Bias of Performance Models**

The steps followed to conduct a local calibration are summarized in four main stages. The AASHTOWare Pavement ME Design 2.5.5 Software was used to compute predicted distress values for selected pavements, based on local specifications. These predictions are based on global calibration coefficients. Based on the selected sections and the months of the latest condition surveys carried out, the predicted distress values are extracted for the

same months as for the latest measured values (Table 5-2). The actual measurements and the predictions are then tabulated together.

### **5.2.1 Elimination of Local Bias for Permanent Deformation Model**

For the rutting analysis, the software computes rutting values for each structural layer separately. Hence the ratio of predicted rutting of each layer to the total rutting was calculated based on predicted values. These ratios were then used to distribute the measured rutting to each individual layer. This was done since no measured rutting values are available for individual layers; only total rutting values are measured. To measure rutting in individual layers, transverse trenches must be cut in the road section. For obvious reason, no trenching was done on any of the road sections selected for calibration. A simple linear regression with no intercept was performed with:

- $y =$  measured values
- $x =$  predicted values.

This is required to fit the regression line through the origin and thus yield calibration coefficients for each of the following layers:

1. Asphalt layer regression coefficient ( $\beta_{1r}$ ).
2. Unbound Base Layer ( $\beta_{s1GB}$ )
3. Subgrade Layer ( $\beta_{s1SG}$ )

The other two calibration factors;  $\beta_{2r}$  and  $\beta_{3r}$  for temperature and load repetitions, consecutively, are kept constant at a value of 1.

The rutting values on each individual layers are then subject to a statistical analysis by calculating:

- a) the mean, maximum value, minimum value and standard deviation
- b) the residuals, the squared error, the sum of squared error (SSE) and the standard error of estimate (SEE).

The results are given in Tables 5-4 and 5-5. The calibration factors were then used to calibrate the model by multiplying the predicted rutting values with the calibration coefficients to obtain the calibrated prediction values. This procedure was done for each structural layer. The value of SSE decreases relative to the SSE obtained with the global calibration. This proves that an optimization effort has been performed.

<b>Rutting</b>	<b>Global SSE</b>	<b>Local SSE</b>
<b>AC Layer</b>	7.809	6.253
<b>Base</b>	3.483	2.744
<b>Subgrade</b>	41.701	36.135
<b>Total Rutting</b>	122.715	102.701

Table 5-4 Sum of Squared Error Computations

<b>Structural Layer</b>	<b>Performance Model</b>	<b>Calibration factor</b>
<b>AC Layer</b>	$\Delta\rho_{AC} = \beta_{1r}k_z\varepsilon_r(HMA)10^{k_{1r}}N^{k_{2r}}\beta_{2r}T^{k_{3r}}\beta_{3r}$	$\beta_{1r} = 1.1731$
<b>Base Layer</b>	$\Delta\rho_{soil} = \beta_{s1}k_{s1}\left(\frac{\varepsilon_0}{\varepsilon_r}\right)e^{-\left(\frac{\rho}{N}\right)^\beta}\varepsilon_v h_{soil}$	$\beta_{s1GB} = 1.2006$
<b>Subgrade</b>	$\Delta\rho_{soil} = \beta_{s1}k_{s1}\left(\frac{\varepsilon_0}{\varepsilon_r}\right)e^{-\left(\frac{\rho}{N}\right)^\beta}\varepsilon_v h_{soil}$	$\beta_{s1SG} = 1.1557$

Table 5-5 Local Calibration Coefficients

Subsequently, the adjusted predicted total rutting is calculated by adding the calibrated values for individual layers given in Table 5-5. The residual error is then calculated for actual total rutting and predicted total rutting. Finally, measured rutting values are then plotted, separately, against both predicted rutting values from global and

local calibration, separately for each layer and for the total rutting. The final plot is to highlight the residuals plot against predicted rutting values.

Tables 5-6 to 5-10 represent the calibration calculations and are used to create the plots in Figures 5-1 and 5-3 to 5-10.

No.	Project	Section No.	Initial		Final		Global			Local			
			Chainage	Chainage	Date of Survey	Age (Mnths)	Actual Ac	Predicted Ac	Error	Error Squared	Predicted Ac	Error	Error Squared
1	E18-1-Inbound	1	0	500	10/01/2013	50	2.340	1.179	-1.161	1.347	1.383	-0.957	0.915
2	E18-1-Inbound	11	5000	5500	10/01/2013	50	2.507	1.179	-1.328	1.764	1.383	-1.124	1.264
3	E18-1-Outbound	54	26500	27000	10/01/2013	50	1.584	1.140	-0.444	0.198	1.337	-0.247	0.061
4	E18-1-Outbound	60	29500	30000	10/01/2013	50	1.648	1.140	-0.508	0.258	1.337	-0.311	0.097
5	E18-1-Inbound	3	1000	1500	10/01/2013	50	2.110	1.179	-0.931	0.867	1.383	-0.727	0.529
6	E99-Inbound	25	12000	12500	10/01/2013	170	1.708	1.971	0.263	0.069	2.312	0.604	0.365
7	E311-Inbound	25	12000	12500	10/01/2013	110	1.020	1.359	0.339	0.115	1.594	0.575	0.330
8	E99-Outbound	19	9000	9500	10/01/2013	170	2.097	1.971	-0.126	0.016	2.312	0.215	0.046
9	E311-Outbound	39	19000	19500	10/01/2013	110	0.758	1.504	0.746	0.557	1.764	1.006	1.013
10	E311-Outbound	105	52000	52500	19/03/2014	124	1.125	1.547	0.422	0.178	1.815	0.690	0.476
11	E311-Inbound	115	57000	57500	19/03/2014	124	1.507	1.397	-0.110	0.012	1.639	0.132	0.017
12	E311-Outbound	43	21000	21500	19/03/2014	124	1.615	1.547	-0.068	0.005	1.815	0.200	0.040
13	E99-Outbound	9	4000	4500	07/04/2014	185	2.753	2.009	-0.744	0.554	2.357	-0.396	0.157
14	E18-2-Outbound	77	38000	38500	07/04/2014	72	1.141	1.313	0.172	0.030	1.540	0.400	0.160
15	E18-2-Outbound	41	20000	20500	07/04/2014	72	1.704	1.313	-0.391	0.153	1.540	-0.164	0.027
16	E311-Inbound	47	23000	23500	08/12/2017	168	1.665	1.516	-0.149	0.022	1.778	0.114	0.013
17	E311-Outbound	93	46000	46500	08/12/2017	168	1.656	1.694	0.038	0.001	1.987	0.331	0.110
18	E99-Inbound	21	10000	10500	10/12/2017	228	2.284	2.151	-0.133	0.018	2.523	0.240	0.057
19	E99-Inbound	19	9000	9500	10/12/2017	228	3.132	2.151	-0.981	0.962	2.523	-0.608	0.370
20	E99-Outbound	1	0	500	17/12/2017	228	2.978	2.151	-0.827	0.683	2.523	-0.454	0.206

Global	Mean Error	-0.296
Global	SSE	7.809
Global	SEE	0.625
Local	Mean Error	-0.024
Local	SSE	6.253
Local	SEE	0.589416

B1r	1.1731
-----	--------

Table 5-6 Computation of Calibration Coefficient  $\beta_{1r}$

No.	Project	Section No.	Initial	Final	Date of Survey	Age (Mnths)	Actual B	Global	Error	Squared Error	Local	Error	Squared Error
			Chainage	Chainage				Predicted B			Predicted B		
1	E18-1-Inbound	1	0	500	10/01/2013	50	1.669	0.841	-0.828	0.686	1.010	-0.659	0.435
2	E18-1-Inbound	11	5000	5500	10/01/2013	50	1.788	0.841	-0.947	0.898	1.010	-0.779	0.606
3	E18-1-Outbound	54	26500	27000	10/01/2013	50	1.024	0.737	-0.287	0.083	0.885	-0.140	0.019
4	E18-1-Outbound	60	29500	30000	10/01/2013	50	1.066	0.737	-0.329	0.108	0.885	-0.181	0.033
5	E18-1-Inbound	3	1000	1500	10/01/2013	50	1.505	0.841	-0.664	0.441	1.010	-0.496	0.246
6	E99-Inbound	25	12000	12500	10/01/2013	170	1.089	1.257	0.168	0.028	1.509	0.420	0.176
7	E311-Inbound	25	12000	12500	10/01/2013	110	0.467	0.622	0.155	0.024	0.747	0.280	0.078
8	E99-Outbound	19	9000	9500	10/01/2013	170	1.337	1.257	-0.080	0.006	1.606	0.268	0.072
9	E311-Outbound	39	19000	19500	10/01/2013	110	0.489	0.970	0.481	0.232	1.165	0.676	0.457
10	E311-Outbound	105	52000	52500	19/03/2014	124	0.715	0.983	0.268	0.072	1.180	0.465	0.217
11	E311-Inbound	115	57000	57500	19/03/2014	124	0.680	0.630	-0.050	0.002	0.756	0.077	0.006
12	E311-Outbound	43	21000	21500	19/03/2014	124	1.026	0.983	-0.043	0.002	1.180	0.154	0.024
13	E99-Outbound	9	4000	4500	07/04/2014	185	1.736	1.267	-0.469	0.220	1.521	-0.215	0.046
14	E18-2-Outbound	77	38000	38500	07/04/2014	72	0.673	0.775	0.102	0.010	0.930	0.257	0.066
15	E18-2-Outbound	41	20000	20500	07/04/2014	72	1.006	0.775	-0.231	0.053	0.930	-0.076	0.006
16	E311-Inbound	47	23000	23500	08/12/2017	168	0.717	0.653	-0.064	0.004	0.784	0.067	0.004
17	E311-Outbound	93	46000	46500	08/12/2017	168	0.996	1.019	0.023	0.001	1.223	0.227	0.052
18	E99-Inbound	21	10000	10500	10/12/2017	228	1.386	1.306	-0.080	0.006	1.568	0.181	0.033
19	E99-Inbound	19	9000	9500	10/12/2017	228	1.901	1.306	-0.595	0.355	1.568	-0.333	0.111
20	E99-Outbound	1	0	500	17/12/2017	228	1.808	1.306	-0.502	0.252	1.568	-0.240	0.058

Global	Mean Error	-0.199
Global	SSE	3.483
Global	SEE	0.417
Local	Mean Error	-0.002
Local	SSE	2.744
Local	SEE	0.390465

Bs1GB	1.2006
-------	--------

Table 5-7 Computation of Calibration Coefficient  $\beta_{s1GB}$

No.	Project	Section No.	Initial	Final	Date of Survey	Age (Mnths)	Actual Sg	Global			Local		
			Chainage	Chainage				Predicted Sg	Error	Squared Error	Predicted Sg	Error	Squared Error
1	E18-1-Inbound	1	0	500	10/01/2013	50	5.977	3.012	-2.965	8.793	3.481	-2.496	6.231
2	E18-1-Inbound	11	5000	5500	10/01/2013	50	6.405	3.012	-3.393	11.513	3.481	-2.924	8.550
3	E18-1-Outbound	54	26500	27000	10/01/2013	50	3.989	2.870	-1.119	1.252	3.317	-0.672	0.452
4	E18-1-Outbound	60	29500	30000	10/01/2013	50	4.149	2.870	-1.279	1.636	3.317	-0.832	0.693
5	E18-1-Inbound	3	1000	1500	10/01/2013	50	5.391	3.012	-2.379	5.659	3.481	-1.910	3.648
6	E99-Inbound	25	12000	12500	10/01/2013	170	2.804	3.236	0.432	0.186	3.740	0.936	0.875
7	E311-Inbound	25	12000	12500	10/01/2013	110	2.514	3.350	0.836	0.700	3.872	1.358	1.844
8	E99-Outbound	19	9000	9500	10/01/2013	170	3.443	3.236	-0.207	0.043	3.740	0.297	0.088
9	E311-Outbound	39	19000	19500	10/01/2013	110	2.003	3.975	1.972	3.888	4.594	2.591	6.712
10	E311-Outbound	105	52000	52500	19/03/2014	124	2.931	4.031	1.100	1.211	4.659	1.728	2.986
11	E311-Inbound	115	57000	57500	19/03/2014	124	3.663	3.396	-0.267	0.072	3.925	0.261	0.068
12	E311-Outbound	43	21000	21500	19/03/2014	124	4.209	4.031	-0.178	0.032	4.659	0.450	0.203
13	E99-Outbound	9	4000	4500	07/04/2014	185	4.493	3.279	-1.214	1.475	3.790	-0.704	0.495
14	E18-2-Outbound	77	38000	38500	07/04/2014	72	2.639	3.038	0.399	0.159	3.511	0.872	0.761
15	E18-2-Outbound	41	20000	20500	07/04/2014	72	3.944	3.038	-0.906	0.820	3.511	-0.432	0.187
16	E311-Inbound	47	23000	23500	08/12/2017	168	3.883	3.536	-0.347	0.120	4.087	0.204	0.041
17	E311-Outbound	93	46000	46500	08/12/2017	168	4.101	4.196	0.095	0.009	4.849	0.748	0.560
18	E99-Inbound	21	10000	10500	10/12/2017	228	3.600	3.391	-0.209	0.044	3.919	0.319	0.102
19	E99-Inbound	19	9000	9500	10/12/2017	228	4.937	3.391	-1.546	2.390	3.919	-1.018	1.036
20	E99-Outbound	1	0	500	17/12/2017	228	4.694	3.391	-1.303	1.699	3.919	-0.775	0.601

Global	Mean Error	-0.624
Global	SSE	41.701
Global	SEE	1.444
Local	Mean Error	-0.100
Local	SSE	36.135
Local	SEE	1.417

<b>Bs1SG</b>	<b>1.1557</b>
--------------	---------------

Table 5-8 Computation of Calibration Coefficient  $\beta s1SG$

No.	Project	Section No.	Initial Chainage	Final Chainage	Date of Survey	Age (Mnths)	Actual Ac	Global Predicted Ac	Global Predicted B	Global Predicted Sg	Total Global Predicted	Error	Squared Error
1	E18-1-Inbound	1	0	500	10/01/2013	50	9.990	1.179	0.841	3.012	5.032	-4.958	24.582
2	E18-1-Inbound	11	5000	5500	10/01/2013	50	10.705	1.179	0.841	3.012	5.032	-5.673	32.183
3	E18-1-Outbound	54	26500	27000	10/01/2013	50	6.595	1.140	0.737	2.870	4.747	-1.848	3.415
4	E18-1-Outbound	60	29500	30000	10/01/2013	50	6.860	1.140	0.737	2.870	4.747	-2.113	4.465
5	E18-1-Inbound	3	1000	1500	10/01/2013	50	9.010	1.179	0.841	3.012	5.032	-3.978	15.824
6	E99-Inbound	25	12000	12500	10/01/2013	170	5.600	1.971	1.257	3.236	6.464	0.864	0.746
7	E311-Inbound	25	12000	12500	10/01/2013	110	4.000	1.359	0.622	3.350	5.331	1.331	1.772
8	E99-Outbound	19	9000	9500	10/01/2013	170	6.875	1.971	1.257	3.236	6.464	-0.411	0.169
9	E311-Outbound	39	19000	19500	10/01/2013	110	3.250	1.504	0.970	3.975	6.449	3.199	10.234
10	E311-Outbound	105	52000	52500	19/03/2014	124	4.770	1.547	0.983	4.031	6.561	1.791	3.208
11	E311-Inbound	115	57000	57500	19/03/2014	124	5.850	1.397	0.630	3.396	5.423	-0.427	0.182
12	E311-Outbound	43	21000	21500	19/03/2014	124	6.850	1.547	0.983	4.031	6.561	-0.289	0.084
13	E99-Outbound	9	4000	4500	07/04/2014	185	8.980	2.009	1.267	3.279	6.555	-2.425	5.881
14	E18-2-Outbound	77	38000	38500	07/04/2014	72	4.450	1.313	0.775	3.038	5.126	0.676	0.457
15	E18-2-Outbound	41	20000	20500	07/04/2014	72	6.650	1.313	0.775	3.038	5.126	-1.524	2.323
16	E311-Inbound	47	23000	23500	08/12/2017	168	6.265	1.516	0.653	3.536	5.705	-0.560	0.314
17	E311-Outbound	93	46000	46500	08/12/2017	168	6.750	1.694	1.019	4.196	6.909	0.159	0.025
18	E99-Inbound	21	10000	10500	10/12/2017	228	7.270	2.151	1.306	3.391	6.848	-0.422	0.178
19	E99-Inbound	19	9000	9500	10/12/2017	228	9.970	2.151	1.306	3.391	6.848	-3.122	9.747
20	E99-Outbound	1	0	500	17/12/2017	228	9.480	2.151	1.306	3.391	6.848	-2.632	6.927

Mean Error	-1.118
SSE	122.715
SEE	2.61103

Table 5-9 Computation of Total Rutting Using Global Calibration



No.	Project	Section No.	Initial Chainage	Final Chainage	Date of Survey	Age (Mnths)	Actual	Local Predicted Ac	Local Predicted B	Local Predicted Sg	Total Predicted	Error	Squared Error
1	E18-1-Inbound	1	0	500	10/01/2013	50	9.990	1.383	1.010	3.481	5.874	-4.116	16.943
2	E18-1-Inbound	11	5000	5500	10/01/2013	50	10.705	1.383	1.010	3.481	5.874	-4.831	23.340
3	E18-1-Outbound	54	26500	27000	10/01/2013	50	6.595	1.337	0.885	3.317	5.539	-1.056	1.115
4	E18-1-Outbound	60	29500	30000	10/01/2013	50	6.860	1.337	0.885	3.317	5.539	-1.321	1.745
5	E18-1-Inbound	3	1000	1500	10/01/2013	50	9.010	1.383	1.010	3.481	5.874	-3.136	9.836
6	E99-Inbound	25	12000	12500	10/01/2013	170	5.600	2.312	1.509	3.740	7.561	1.961	3.846
7	E311-Inbound	25	12000	12500	10/01/2013	110	4.000	1.594	0.747	3.872	6.213	2.213	4.896
8	E99-Outbound	19	9000	9500	10/01/2013	170	6.875	2.312	1.606	3.740	7.658	0.783	0.613
9	E311-Outbound	39	19000	19500	10/01/2013	110	3.250	1.764	1.165	4.594	7.523	4.273	18.258
10	E311-Outbound	105	52000	52500	19/03/2014	124	4.770	1.815	1.180	4.659	7.654	2.884	8.316
11	E311-Inbound	115	57000	57500	19/03/2014	124	5.850	1.639	0.756	3.925	6.320	0.470	0.221
12	E311-Outbound	43	21000	21500	19/03/2014	124	6.850	1.815	1.180	4.659	7.654	0.804	0.646
13	E99-Outbound	9	4000	4500	07/04/2014	185	8.980	2.357	1.521	3.790	7.668	-1.312	1.723
14	E18-2-Outbound	77	38000	38500	07/04/2014	72	4.450	1.540	0.930	3.511	5.982	1.532	2.347
15	E18-2-Outbound	41	20000	20500	07/04/2014	72	6.650	1.540	0.930	3.511	5.982	-0.668	0.446
16	E311-Inbound	47	23000	23500	08/12/2017	168	6.265	1.778	0.784	4.087	6.649	0.384	0.148
17	E311-Outbound	93	46000	46500	08/12/2017	168	6.750	1.987	1.223	4.849	8.060	1.310	1.716
18	E99-Inbound	21	10000	10500	10/12/2017	228	7.270	2.523	1.568	3.919	8.010	0.740	0.548
19	E99-Inbound	19	9000	9500	10/12/2017	228	9.970	2.523	1.568	3.919	8.010	-1.960	3.840
20	E99-Outbound	1	0	500	17/12/2017	228	9.480	2.523	1.568	3.919	8.010	-1.470	2.160

Mean Error	-0.126
SSE	102.701
SEE mm	2.388647

Table 5-10 Computation of Total Rutting Using Local Calibration

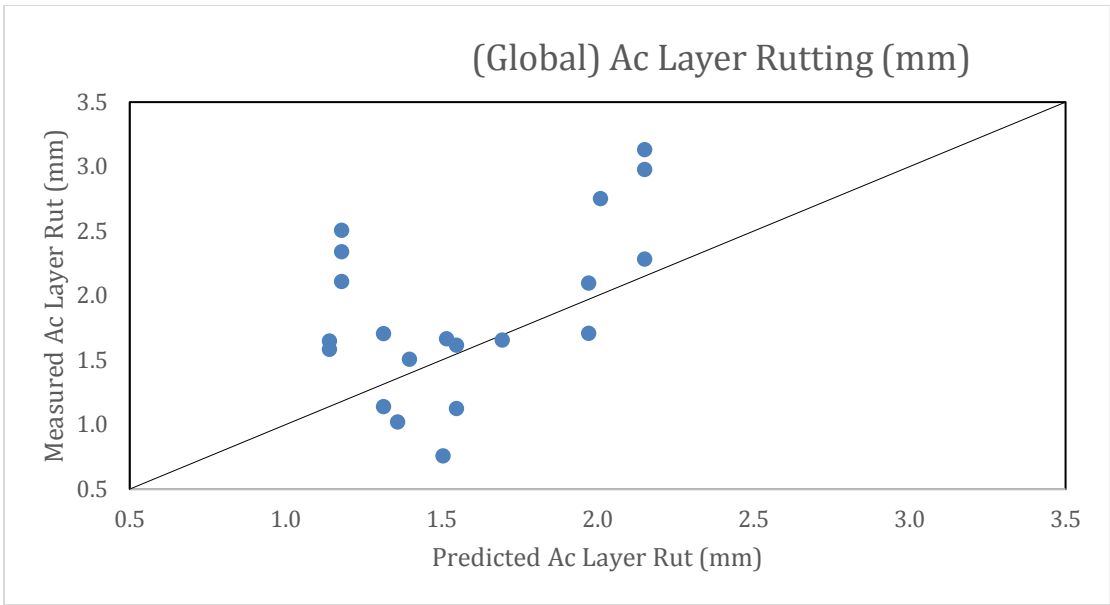


Figure 5-3 Asphalt Layer (Global Calibration)

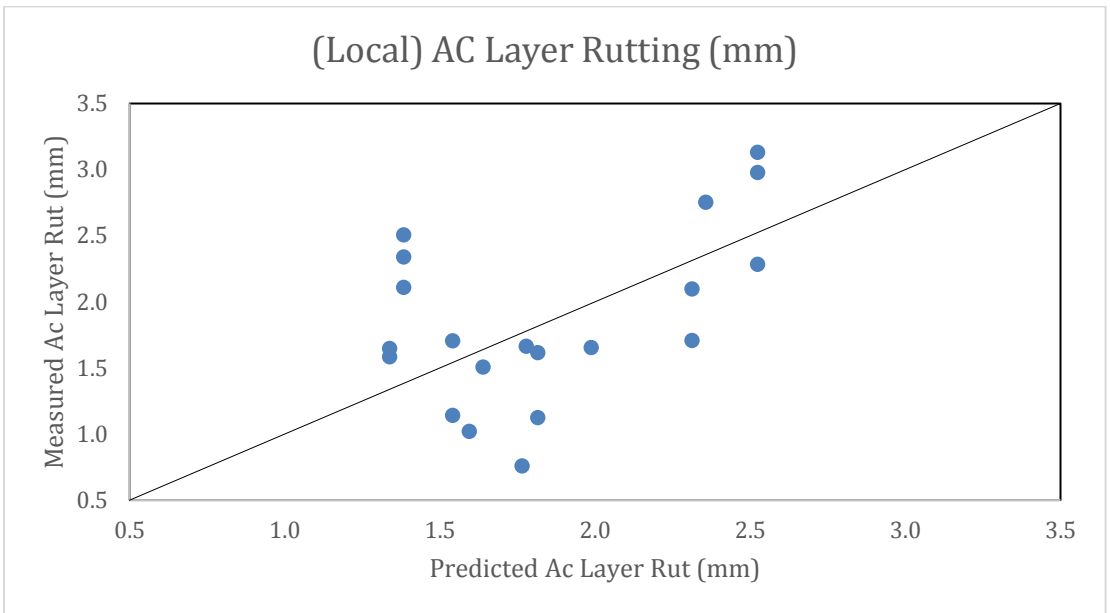


Figure 5-4 Asphalt Layer Rutting (Local Calibration)

Figures 5-3 and 5-4 indicate that the local calibration coefficients have yielded a better fit between the measured and predicted rutting values in the asphalt layer. The plotted values have a better dispersion along the line of equality after local calibration, with an equal number of points above and below the line. This indicates that the local calibration has improved the performance model.

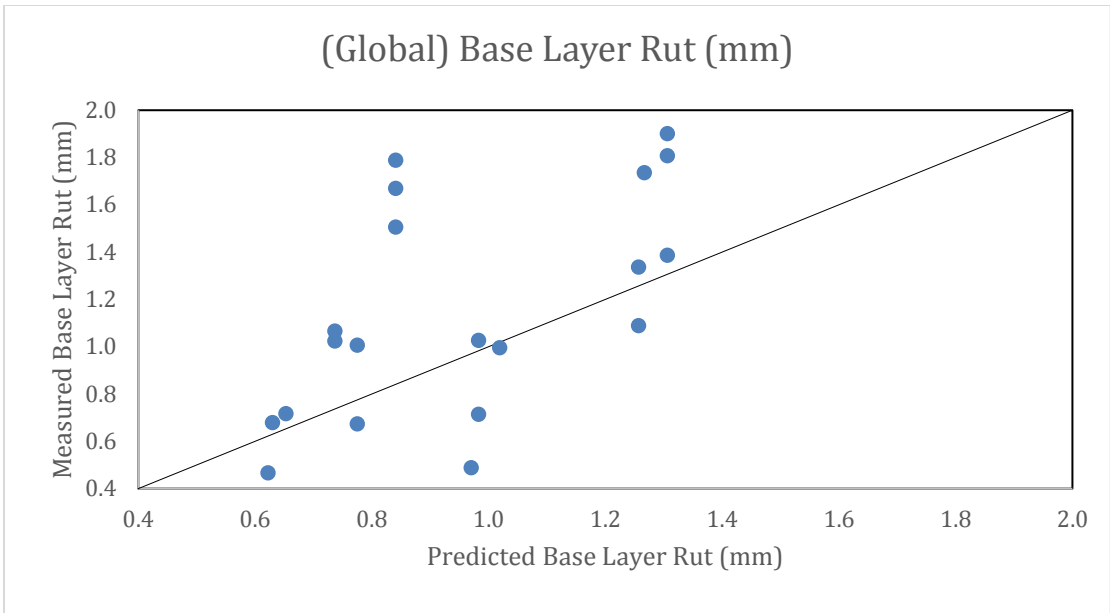


Figure 5-5 Base Layer Rutting (Global Calibration)

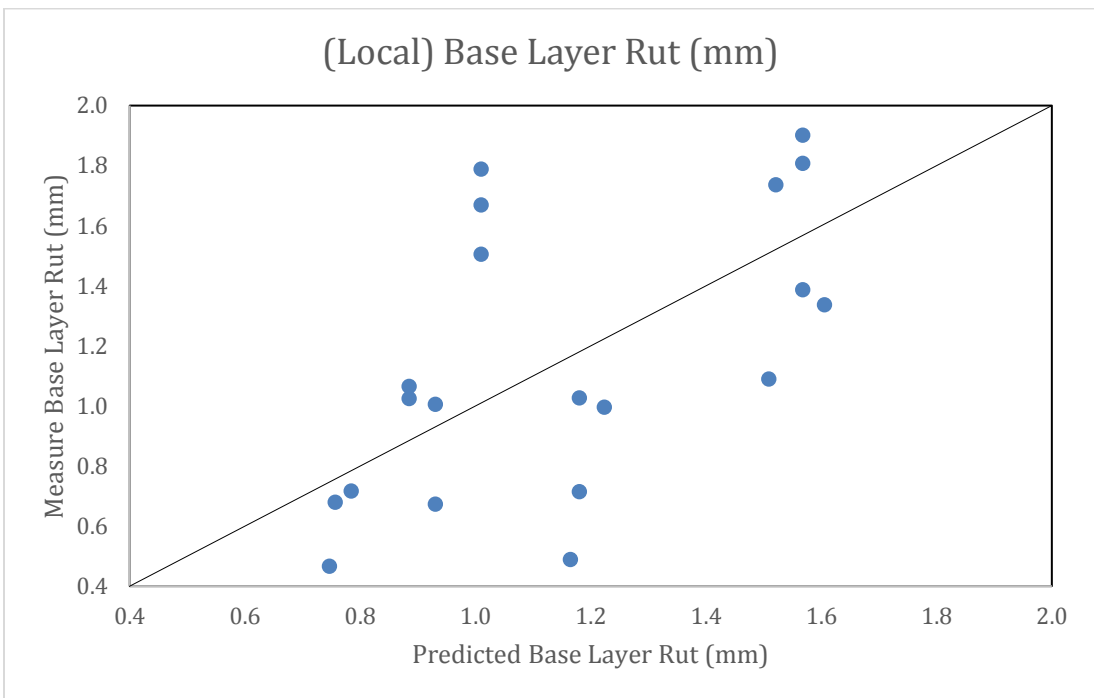


Figure 5-6 Base Layer Rutting (Local Calibration)

Figures 5-5 to 5-8 show the measured versus predicted rutting values in the base and subgrade layers. As for the asphalt layer, the local calibration has improved the prediction of rutting in these two granular layer. The points in Figures 5-6 and 5-8 are

better distributed against the equality line than the corresponding points in Figures 5-5 and 5-7, respectively. However, it seems that the precision in predicting the rutting values has not improved much.

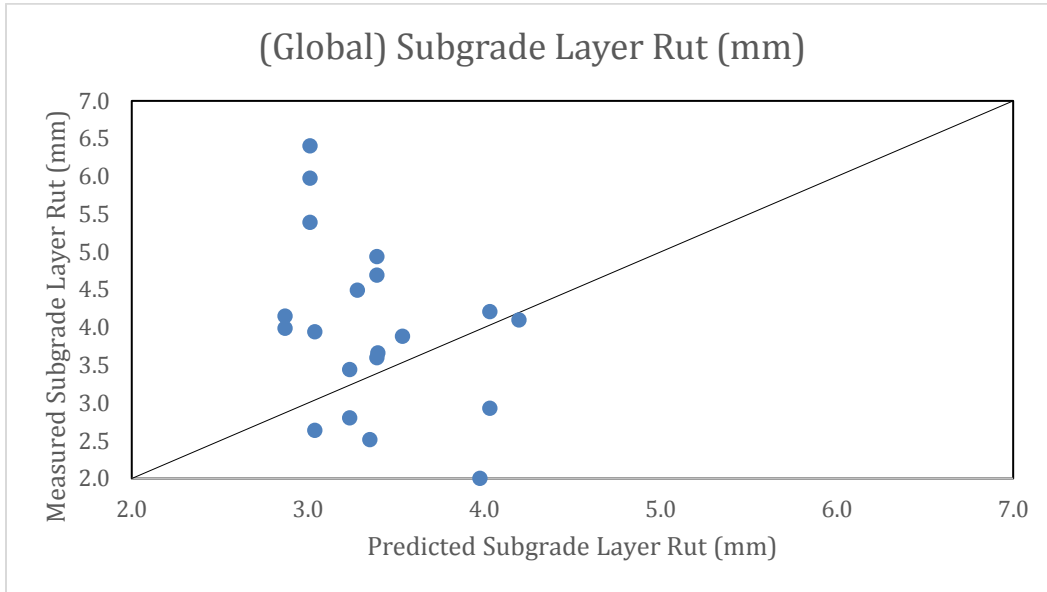


Figure 5-7 Subgrade Layer Rutting (Global Calibration)

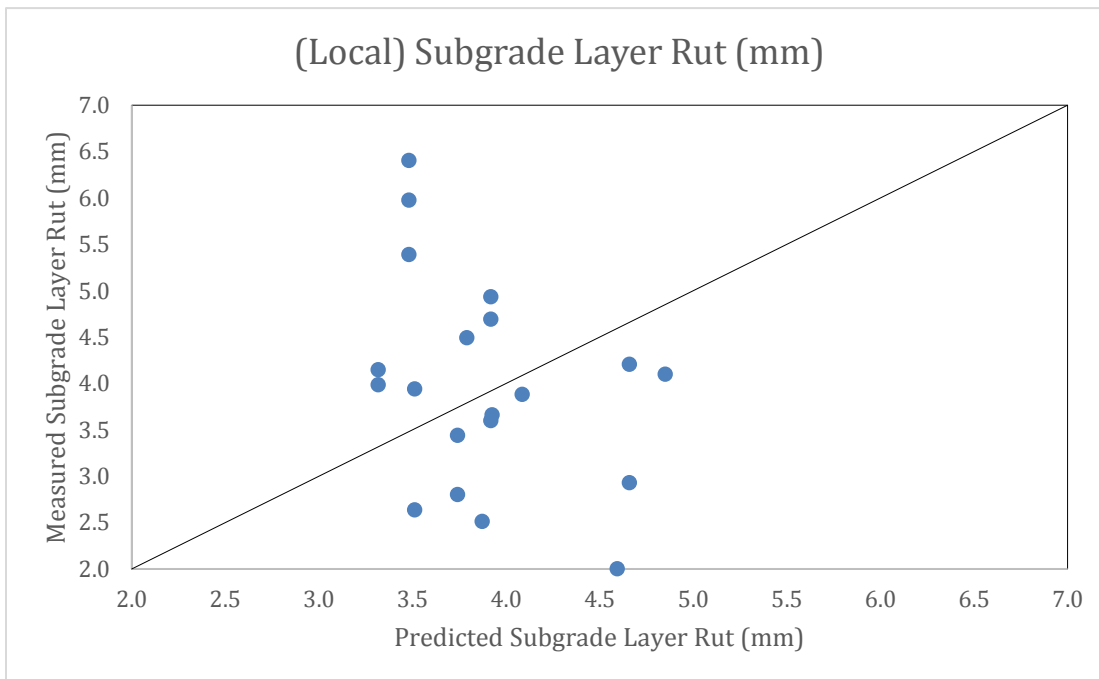


Figure 5-8 Subgrade Layer Rutting (Local Calibration)

The predicted total rutting, calculated as the sum of predicted rutting in the three structural layers, are plotted versus the measured rutting in Figures 5-9 and 5-10. Figure 5-10 shows that the local calibration has improved the prediction of total rutting since the number of points above and below the equality line is about the same.

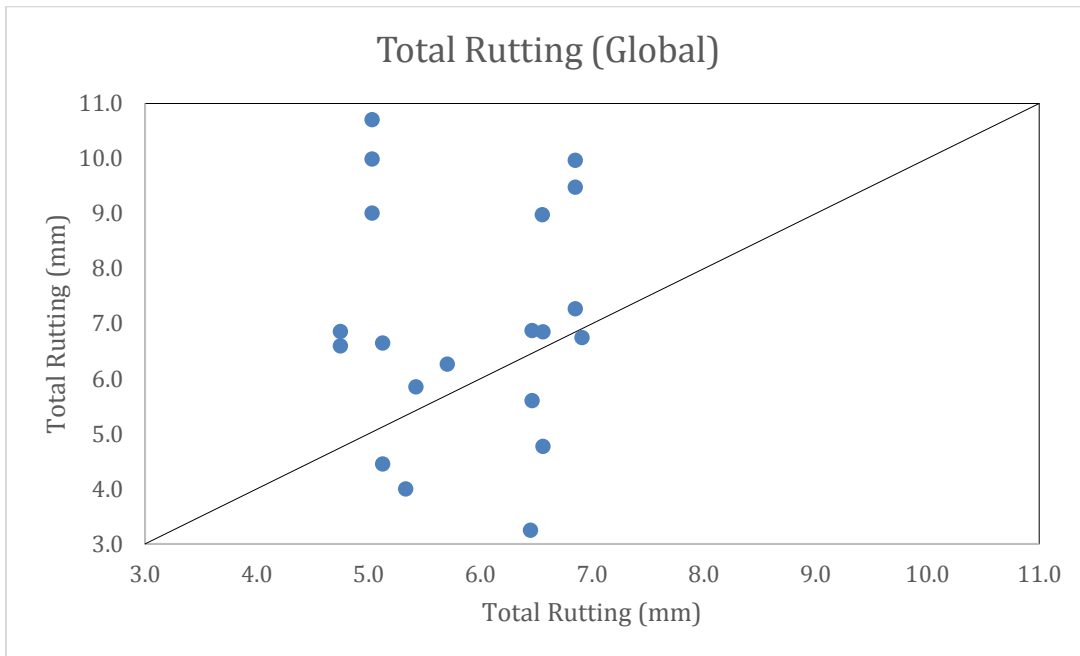


Figure 5-9 Total Rutting (Global Calibration)

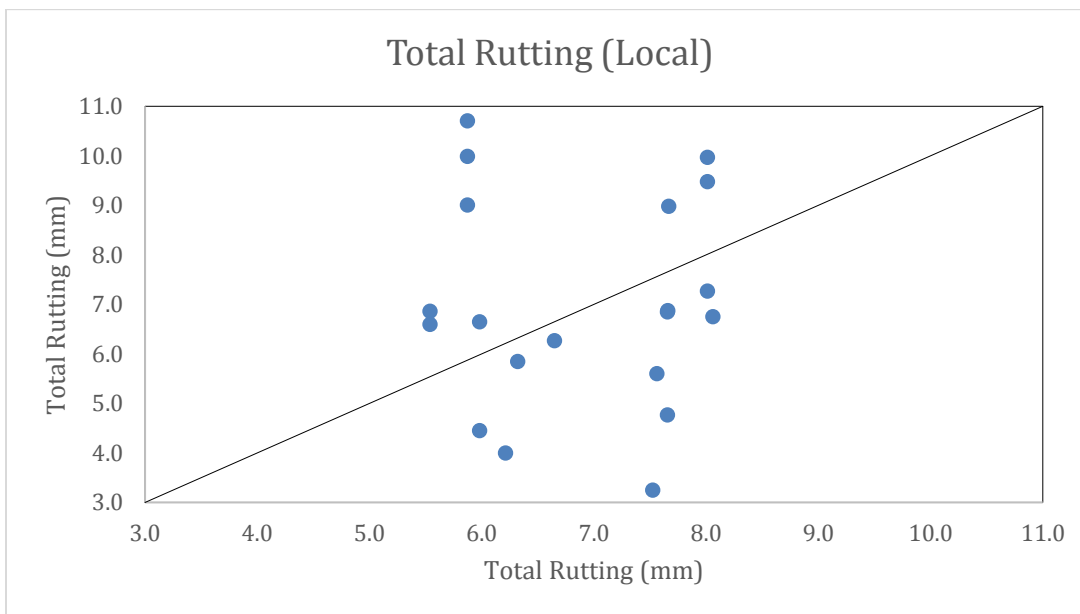


Figure 5-10 Total Rutting (Local Calibration)

Figure 5-11 shows the errors in predicting total rutting versus the predicted values. The Figure indicates that there is no correlation between the errors and the predicted values, suggesting that there is no bias in the total rutting prediction model.

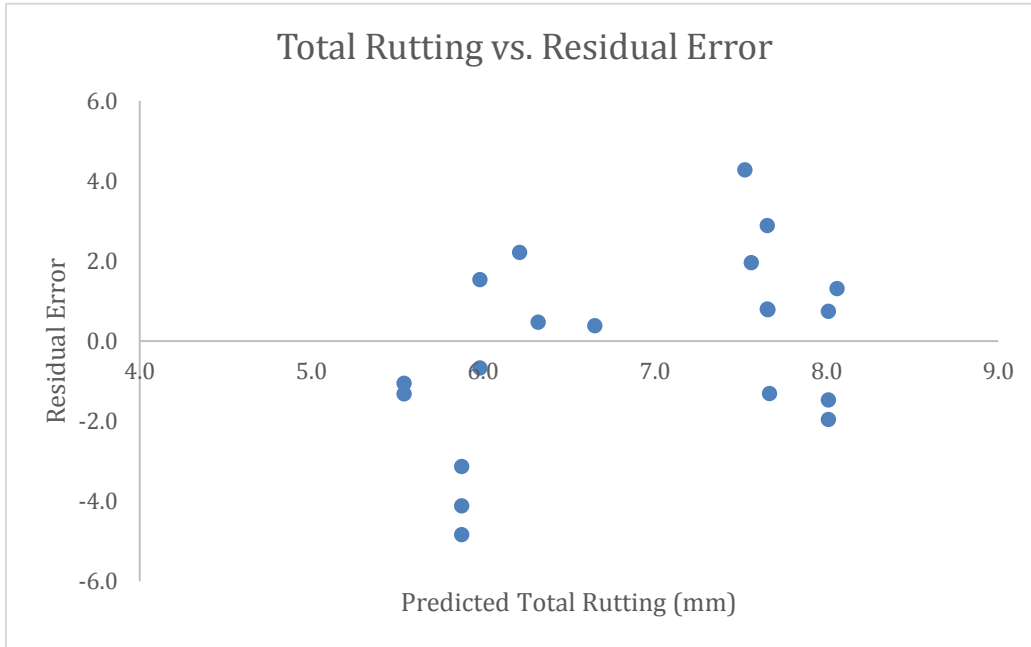


Figure 5-11 Total Rutting vs Residual Error

### **5.2.2 Elimination of Local Bias for IRI Model**

For the IRI analysis, calibration coefficients are required for fatigue cracking, transverse cracking, rut depth and the site factor, as shown in equation 25:

$$IRI = IRI_0 + C_1(RD) + C_2(FC_{Total}) + C_3(TC) + C_4(SF)$$

The following steps were carried out to perform the calibration of the IRI model:

1. A difference between the measured IRI and the Initial IRI was calculated.
2. The software produced predictions for the IRI based on the global coefficients.
3. The total predicted rut depth (RD) was calculated as the sum of predicted rutting for each of the three structural layers.

4. Fatigue cracking and Transverse cracking data was not available and hence were given a value of 0 for all sections

5. The Site Factor (SF) was calculated using Equation 26

$$SF = Age[0.02003(PI + 1) + 0.00794(Precip + 1) + 0.000636(FI + 1)]$$

The calculation of the Site Factor, *SF*, is shown in Table 5-14. The precipitation value was considered as 112 mm/year (4.41 in./year) for all sections.

6. A simple linear regression with no intercept was performed with:

- *y* = measured values of IRI
- *x* = predicted values of RD and SF

This is required to fit the regression line through the origin and obtain calibration coefficients for rut depth and site factor; they are given in Table 5-11, for IRI being measured in in/mile. The other two calibration factors; *C*<sub>2</sub> and *C*<sub>3</sub> for fatigue cracking (FC) and transverse cracking (TC), are kept as 0.0, since cracking is a rare occurrence on asphalt pavements in UAE.

The residuals, the squared error, the sum of squared error (SSE) and the standard error of estimate (SEE) of the IRI model are then calculated. The calibration factors were then used to calibrate the model by using equation 25 to yield calibrated prediction values. The value of SSE decreased after the local calibration computation of SSE (Table 5-12). This proves that the local calibration effort improved the prediction of IRI.

Coefficient	Distress Coefficient	Calibration factor	
		Global	Local
<b><i>C</i><sub>1</sub></b>	for Rut Depth in inches	40	540.3
<b><i>C</i><sub>4</sub></b>	for Site Factor	0.015	-22.583

Table 5-11 Local Calibration Coefficients

Finally, the measured IRI values are then plotted against predicted IRI values from global calibration (Figure 5-11) and from the local calibration (Figure 5-12). The two figures show clearly that the IRI prediction model has improved after the local calibration; the data points are better distributed versus the line of equality.

<b>Global SSE for IRI</b>	<b>Local SSE for IRI</b>
44.184	42.056

*Table 5-12 Sum of Squared Error Computations*

Figure 5-13 shows the residuals plot against predicted IRI values with the locally calibrated model. This figure demonstrates that the errors are equally distributed as positive and negative values, but the absolute values remain quite large. This suggests that the bias has been eliminated, but the precision of IRI prediction has not been improved. A possible improvement of the precision in predicting the IRI is to conduct the local calibration with a larger dataset in which performance data for a larger number of road sections is included. AASHTO (2010) recommends the following sample sizes when calibrating each distress in order to have a better representation of the pavements when performing a local calibration:

- Total rutting: 20 sections
- Load related cracking: 30 sections
- Non load related cracking: 26 sections

In the case of IRI in this research, only 20 sections were used to perform the calibration and this explain the poor precision in predicting the IRI.



No.	Project	Actual IRI	Initial IRI	Actual Adjusted(m/km)	Global IRI (m/km)	Error	Error^2	Local IRI (m/km)	Error	Error^2
1	E18-1-Inbound	3.90	1.00	2.90	1.15	-1.75	3.0625	1.639	-1.261	1.59
2	E18-1-Inbound	3.72	1.00	2.72	1.15	-1.57	2.4649	1.639	-1.081	1.17
3	E18-1-Outbound	4.93	1.00	3.93	1.14	-2.79	7.7841	1.542	-2.388	5.70
4	E18-1-Outbound	4.44	1.00	3.44	1.14	-2.30	5.2900	1.542	-1.898	3.60
5	E18-1-Inbound	4.12	1.00	3.12	1.15	-1.97	3.8809	1.639	-1.481	2.19
6	E99-Inbound	2.08	1.00	1.08	1.44	0.36	0.1296	1.512	0.432	0.19
7	E311-Inbound	1.31	1.00	0.31	1.23	0.92	0.8409	1.703	1.390	1.93
8	E99-Outbound	1.93	1.00	0.93	1.44	0.51	0.2601	1.512	0.582	0.34
9	E311-Outbound	1.70	1.00	0.70	1.26	0.56	0.3136	2.078	1.378	1.90
10	E311-Outbound	1.26	1.00	0.26	1.30	1.04	1.0878	2.109	1.852	3.43
11	E311-Inbound	2.03	1.00	1.03	1.26	0.23	0.0511	1.727	0.693	0.48
12	E311-Outbound	2.52	1.00	1.52	1.30	-0.22	0.0475	2.109	0.591	0.35
13	E99-Outbound	2.50	1.00	1.50	1.49	-0.01	0.0001	1.499	-0.001	0.00
14	E18-2-Outbound	2.30	1.00	1.30	1.17	-0.13	0.0169	1.662	0.362	0.13
15	E18-2-Outbound	5.90	1.00	4.90	1.17	-3.73	13.9129	1.662	-3.238	10.49
16	E311-Inbound	1.66	1.00	0.66	1.34	0.68	0.4624	1.800	1.140	1.30
17	E311-Outbound	1.29	1.00	0.29	1.39	1.10	1.2100	2.203	1.913	3.66
18	E99-Inbound	2.40	1.00	1.40	1.59	0.19	0.0361	1.470	0.070	0.00
19	E99-Inbound	4.28	1.00	3.28	1.59	-1.69	2.8561	1.470	-1.810	3.28
20	E99-Outbound	1.90	1.00	0.90	1.59	0.69	0.4761	1.470	0.570	0.32

Mean Error Global	-1.49
Mean Error Local	-0.62
SSE Global	44.184
SSE Local	42.056
SEE Local	1.567
SEE Global	1.529

<b>C1</b>	540.3352
<b>C4</b>	-22.5828

Table 5-13 Computation of IRI Using Global and Local Calibrations

No.	Roadway	Section	Chainage Initial	Chainage Final	Condition Survey	Age	PI	FI	Precepitation (in)	SF
1	E18-1-Inbound	1	0	500	10/01/2013	5	0	0	4.41	0.14
2	E18-1-Inbound	11	5000	5500	10/01/2013	5	0	0	4.41	0.14
3	E18-1-Outbound	54	26500	27000	10/01/2013	5	0	0	4.41	0.14
4	E18-1-Outbound	60	29500	30000	10/01/2013	5	0	0	4.41	0.14
5	E18-1-Inbound	3	1000	1500	10/01/2013	5	0	0	4.41	0.14
6	E99-Inbound	25	12000	12500	10/01/2013	15	5	0	4.41	1.85
7	E311-Inbound	25	12000	12500	10/01/2013	10	0	0	4.41	0.24
8	E99-Outbound	19	9000	9500	10/01/2013	15	5	0	4.41	1.85
9	E311-Outbound	39	19000	19500	10/01/2013	10	0	0	4.41	0.24
10	E311-Outbound	105	52000	52500	19/03/2014	11	0	0	4.41	0.26
11	E311-Inbound	115	57000	57500	19/03/2014	11	0	0	4.41	0.26
12	E311-Outbound	43	21000	21500	19/03/2014	11	0	0	4.41	0.26
13	E99-Outbound	9	4000	4500	07/04/2014	16	5	0	4.41	1.97
14	E18-2-Outbound	77	38000	38500	07/04/2014	6	0	0	4.41	0.16
15	E18-2-Outbound	41	20000	20500	07/04/2014	6	0	0	4.41	0.16
16	E311-Inbound	47	23000	23500	08/12/2017	14	0	0	4.41	0.32
17	E311-Outbound	93	46000	46500	08/12/2017	14	0	0	4.41	0.32
18	E99-Inbound	21	10000	10500	10/12/2017	19	5	0	4.41	2.33
19	E99-Inbound	19	9000	9500	10/12/2017	19	5	0	4.41	2.33
20	E99-Outbound	1	0	500	17/12/2017	19	5	0	4.41	2.33

Table 5-14 Computation of Site Factor

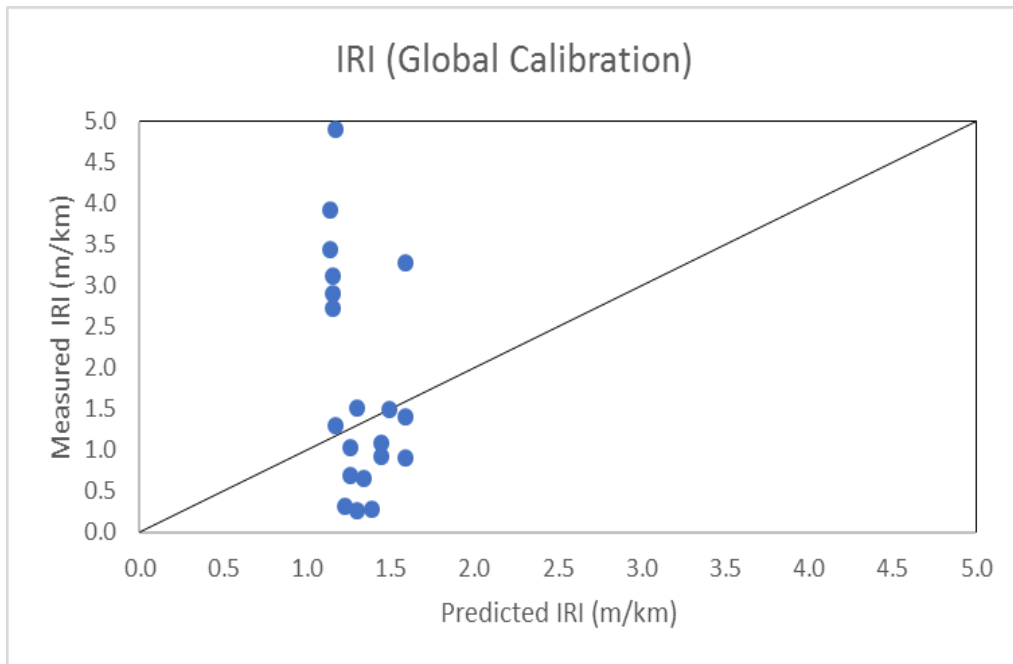


Figure 5-12 IRI (Global Calibration)

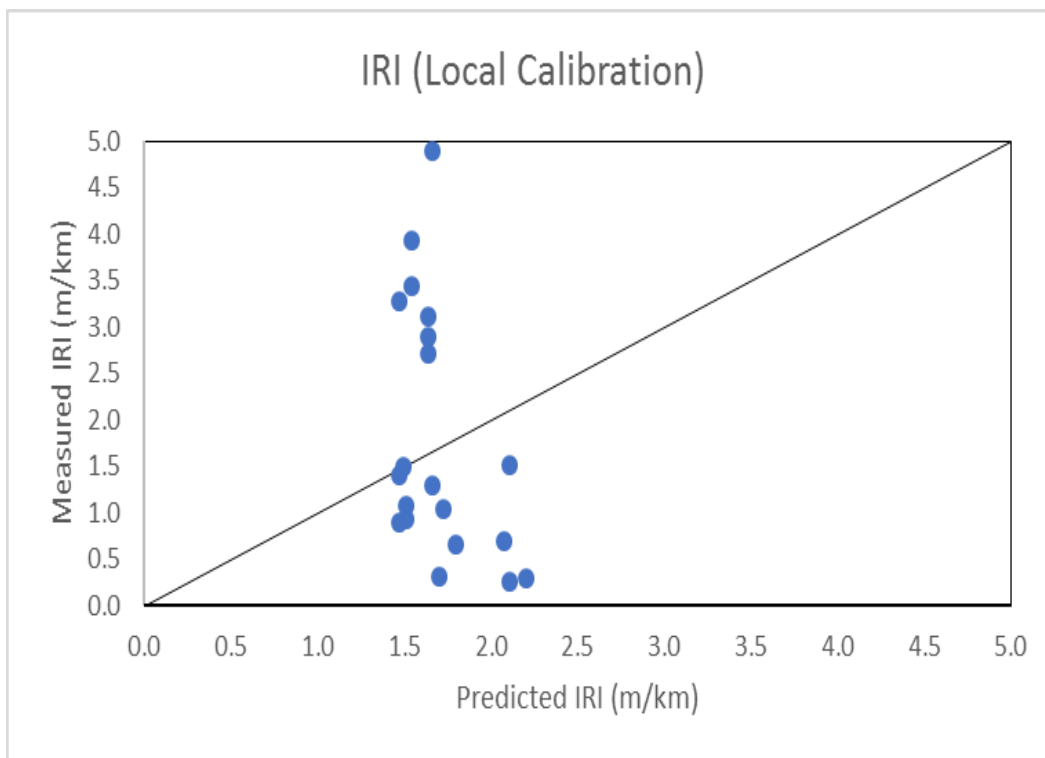


Figure 5-13 IRI (Local Calibration)

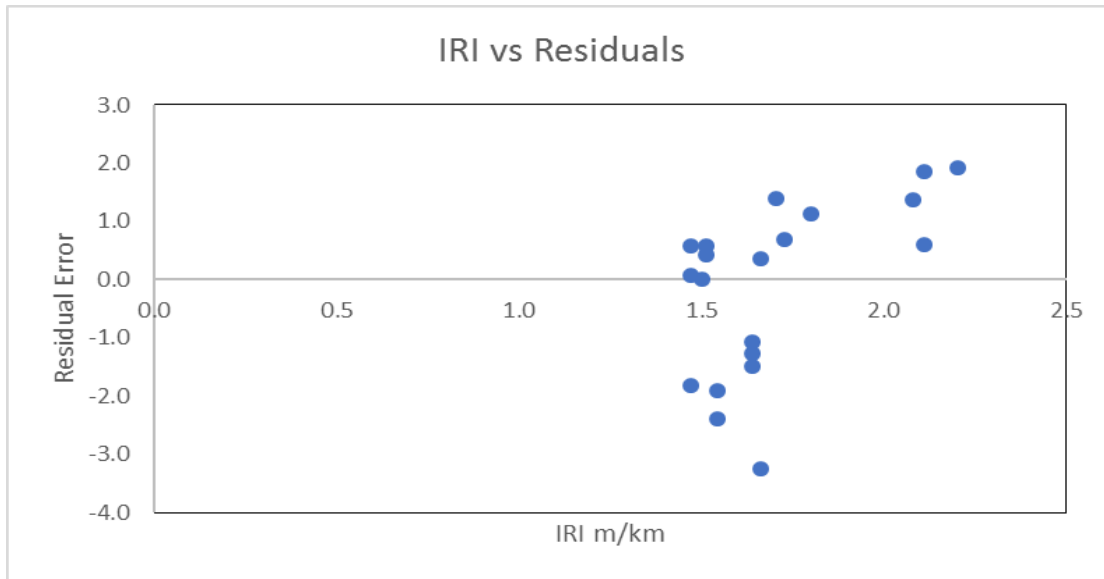


Figure 5-14 IRI vs. Residual Error

### **5.3 Goodness of Fit Statistics**

A Goodness of Fit test is an indicator of prediction accuracy. It computes the standard error of estimate (SEE) from both the global and the local calibrations. An evaluation is performed between the results obtained and the global criteria in Table 5-15. A comparison is then carried out between the results to assess the improvement to the performance model brought by the local calibration.

According to AASHTO (2010) and referring to the global criteria at the start of the chapter, a reasonable SEE for rutting is set at 0.1in, or 2.54mm. It is observed from the Table 5-15 that the local calibration has produced a very reasonable SEE at 2.39 mm, with an improvement from 2.61 mm for the global calibration. This highlights that local calibration has improved the prediction of total rutting.

AASHTO (2010) recommends a reasonable SEE value of 0.268 m/km (17 in/mi) for the IRI. The SEE obtained for the predicted values in local calibration is 1.53 m/km,

which is an improvement from 1.567 m/km obtained in the global calibration. However, the value is much larger than the desired precision of 0.268 m/km. This indicates that the IRI model is not precise. Therefore, it is recommended that the IRI model calibration be done again with a more extensive pavement performance dataset, when available.

Performance Model	Mean Error ( $e_r$ )		Standard Error of Estimate (SEE)	
	Global	Local	Global	Local
<b>Total Rutting</b>	-1.118 mm	-0.126	2.61 mm	2.39 mm
<b>IRI</b>	-0.49 m/km	0.0 m/km	1.567 m/km	1.53 m/km

Table 5-15 Mean Error and SEE for Global and Local Calibration

## **Chapter 6 Summary, Conclusion and Recommendations**

### **6.1 Summary and Conclusion**

The MEPDG rutting and roughness models for new flexible pavement structures has been calibrated to accommodate local conditions in the United Arab Emirates. The calibration dataset included performance data collected 20 flexible pavement sections. The AASHTOWare Pavement ME 2.5.5 software has been used to compute the predicted distress values using the global calibration coefficients currently incorporated in the software. Pavement structural design and materials properties, traffic design attributes, counts and WIM data and lastly, local climate data have been used to perform the local calibration. The data was supplied by MOID, with some specific input values being acquired from the ADM Roadway Design Manual (2014). The climate information was obtained from the NCMS website.

The AASHTO's Guide for Local Calibration of the Mechanistic-Empirical Pavement Design Guide (2010) was the main reference for the calibration procedure. The decision on pavement section selection was based on roads with at least 15 years since construction. Roadways of different configurations, pavement structures, material properties and subgrade soils were considered. Similar traffic and climate conditions were used for all projects. The performance data was supplied for three condition surveys carried out in 2013, 2014 and 2017.

A regression analysis was performed between the measured distress values and the values predicted by the software's performance model to obtain the calibration coefficients. The calculated local calibration coefficients were then used to re-calculate the predicted distress values (local calibration). These were used to estimate the goodness of fit after the

local calibration. reducing SSE. This reduction achieves more accurate prediction values, resulting in a calibration for local conditions.

Since no performance data were available for alligator and transverse cracking, these models could not be calibrated. Alligator and transverse cracking rarely develops of flexible pavements in the UAE.

Rutting is the major pavement distress in the UAE due to a combination of high temperatures and heavy truck traffic. The predicted rutting using the global model were lower than the measured rutting values. Therefore, a local calibration of the rutting model was needed. The following local calibration coefficients were obtained for the rutting models in the asphalt layer, granular base and subgrade, respectively:

$$\beta_{1r} = 1.1731, \beta_{s1GB} = 1.2006, \beta_{s1SG} = 1.1557$$

Furthermore, the mean error between the measured and the predicted values using local calibration coefficients produced a value of -0.126 mm, compared to -1.118 mm with the global calibration. Finally, a SEE value of 2.267 mm was obtained for the local calibration, which is lower than 2.477 mm obtained with the global calibrated models. The SEE values is less than the values recommended by the AASHTO calibration guide (2.54mm). Therefore, the calibration of the rutting model was successful.

The software with the global calibrated models significantly underestimated the IRI values. Therefore, a local calibration for the IRI model was required. The following local calibration coefficients were obtained for the Rut Depth and Site Factor, respectively:

$$C_1 = 540.33, C_4 = -22.58$$

The SEE in the IRI model has improved from 1.57 m/km for the global calibration to 1.53 m/km for the local calibration, indicating that the IRI prediction model is improved.

However, the SEE which is much higher than the recommended AASHTO criteria of 0.268 m/km (17 in/mile). This indicates that the locally calibrated IRI model is still not precise.

## **6.2 Recommendations**

This research work and the experience accumulated in assembling the calibration dataset led to the following recommendations:

- a) A centralized database that stores, pavement information, pavement design and historical pavement condition survey data for UAE road network is needed. An extensive database is required comprising of historical condition surveys carried out on all roadways constructed, maintained and managed by MOID will provide more data to enhance the accuracy of the calibration effort. It will also provide all the required data to perform calibration for the other models.
- b) To better calibrate rutting models, accurate measurements of rutting in each pavement layer is needed. Therefore, it is recommended that trench studies be conducted to measure rutting in each layer of the pavement.
- c) It was also noticed that pavement section measurements were not uniform in terms of sections length. Better condition survey practice and accurate, uniform pavement distress measurements are required as measured distress values are critical for the calibration process.
- d) To better understand the characteristics of truck traffic in the UAE, more studies should be conducted to collect classification/volume and WIM data. Due to lack of detailed data, the distribution by vehicle class was available only for one location and was used for all pavement sections. Default values were used for other traffic



input values due to their unavailability. This may have contributed to inaccuracy in the prediction of pavement performance.

- e) Regarding climate data, MOID in collaboration with NCMS need to assemble an hourly climate dataset. The two-year hourly dataset used in this research may not represent well the climatic conditions experienced by the pavement sections used in the calibration during their in-service life.

## References

- AASHTO. (2008). *Mechanistic Empirical Pavement Design Guide*. Washington DC: American Association of State Highway and Transportation Officials.
- AASHTO. (2010). *Guide for the Local Calibration of the Mechanistic-Empirical Pavement Design Guide*. Washington DC: American Association of State Highway and Transportation Officials.
- Abdullah, A (2015). *Development of a Simplified Flexible Pavement Design Protocol For New York State Department of Transportation Based on AASHTO ME Pavement Design Guide* . Arlington, TX: University of Texas at Arlington.
- Abu Dhabi Municipality (2014). *Roadway Design Manual*. Abu Dhabi: Department of Municipal Affairs.
- Al Suleiman, T. I., & Shiyab, A. M. (2003, June). Prediction of Pavement Remaining Service Life Using Roughness Data—Case Study in Dubai. *The International Journal of Pavement Engineering*, 4(2), 121-129.
- Arizona Department of Transport (2014). *Calibration and Implementation of the AASHTO Mechanistic-Empirical pavement Design Guide in Arizona*. Champaign, IL: Applied Research Associates .
- ASCE. (2017). *Infrastructure Report Card – Roads*. Available: <https://www.infrastructurereportcard.org/cat-item/roads/>. Last accessed 20<sup>th</sup> Jan 2019.
- Asphalt Institute (1989). *The Asphalt Handbook*. 4th ed. Lexington, KY: Asphalt Institute.

Bhattacharya, B. Von Quintus, H. Darter, M (2015). *Implementation and Local Calibration of the MEPDG Transfer Functions in Wyoming*. Cheyenne, WY: Applied Research Associates.

Coelho, N (2016). *Calibration of MEPDG Performance Models for Flexible Pavement Distresses to Local Conditions of Ontario* Arlington, TX: University of Texas at Arlington.

Dornier Consulting International (2018). *Ground Water Atlas of Abu Dhabi Emirate*. Abu Dhabi: Environment Agency-Abu Dhabi. p48-66

Elbasyouny, M. (2013). *Pavement Design Manual* (Abu Dhabi Department of Transport). Abu Dhabi, United Arab Emirates: Parsons International Limited.

Kasperick, T and Ksaibati, K. (2015). *Calibration of the Mechanistic - Empirical Pavement Design Guide for Local Paved Roads in Wyoming*. *Mountain Plains Consortium*.

Li, Q, Xiao, D, Wang, K, Hall, K and Qiu, Y. (2011). *Mechanistic-empirical pavement design guide (MEPDG): A Bird's Eye View*. *Journal of Modern Transportation*. 19, p114-133.

Maupin, G and Mokarem, D (2006). *Investigation of AASHTO Rut Test Procedure Using the Asphalt Pavement Analyzer*. Richmond, VA: Virginia Department of Transport.

Momin, S (2011). *Local Calibration of Mechanistic Empirical Pavement Design Guide for North Eastern United States*. Arlington, TX: University of Texas at Arlington.

Rauros Group. (2019) *Services Page*. Available: <http://www.raurosgroup.com/Servicios>.

Last accessed 14th Feb 2019.

Read, J and Whiteoak, D (2003). *The Shell Bitumen Handbook*. 5th ed. London, England: Thomas Telford Publishing.

Retherford, J and McDonald, M. (2010). Reliability Methods Applicable to Mechanistic - Empirical Pavement Design Method. *Journal of the Transportation Research Board*. 2154, p130-137.

Robbins, M, Rodezno, C, Tran, N, Timm, D (2017). *Pavement ME Design - Summary of Local Calibration Efforts For Flexible Pavements*. Auburn, AL.: National Center for Asphalt Technology.

Romanoschi, S and Abdullah, A (2017). *Development of a Simplified Flexible Pavement Design Protocol for New York State Department of Transportation Based on the AASHTO Mechanistic - Empirical Pavement Design Guide*. Topeka, KA: Kansas Department of Transportation.

Selvaraj, S. (2007). *Development of Flexible Pavement Rut Prediction Models From The NCAT Test Track Structural Study Sections Data*. Auburn, AL.: University of Auburn.

Von Quintus, H. Schwartz, C. McCuen, R. and Andrei, D. (2003). Jackknife Testing - An Experimental Approach to Refine Model Calibration and Validation. *Transportation Research Board*. 283 (1)

Witczak, M and El-Basyouny, M. (2004). *Appendix II-1: Calibration of Fatigue Cracking Models for Flexible Pavements*. Guide for Mechanistic Empirical Design of New Rehabilitated Pavement Structures. Champaign, IL: Transportation Research Board.

## Acronyms

AADT = Average Annual Daily Traffic

AADTT = Average Annual Daily Truck Traffic

AASHTO = American Association of State Highway and Transportation Officials

E18-1 IB = RAK Airport to Sha'am

E18-2 IB = Manama to RAK Airport

E18-1 OB = Sha'am to RAK Airport

E18-2 OB = RAK Airport to Manama

E311 IB = National Paints Interchange to RAK

E311 OB = RAK to National Paints Interchange

E99 IB = Oman border to Kalba

E99 OB = Kalba to Oman border

ESALS = Equivalent Single Axle Load

FC = Fatigue Cracking

FHWA = Federal Highway Agency

HMA = Hot Mixed Asphalt

IRI = International Roughness Index

MOID = Ministry of Infrastructure Development

RD = Rut Depth

SF = Safety Factor

TC = Transverse Cracking

U.A.E. = United Arab Emirates

## Appendix A – Pavement Distress Data Sets

### A1 - IRI Data Set:

No.	Terrain	Road	Section	Chainage		2013	2014	2017
				From	To	Avg IRI	Avg IRI	Avg IRI
1	M	E18-1 IB	2	1000	1500	4.12	2.71	2.10
2	M	E18-1 IB	4	3000	3500	3.22	2.30	1.45
3	M	E18-1 IB	6	5000	5500	3.72	2.24	1.75
4	M	E18-1 IB	8	7000	7500	3.29	3.14	1.55
5	M	E18-1 IB	16	17500	18000	4.08	3.16	1.50
6	M	E18-1 IB	19	21000	21500	4.42	2.18	1.70
7	M	E18-1 OB	8	26500	27000	4.93	3.02	1.30
8	M	E18-1 OB	11	29500	30000	4.44	3.47	1.26
9	M	E18-2 OB	4	20800	21300	3.24	4.43	1.42
10	M	E18-2 IB	2	14500	14750	3.10	3.52	1.50
11	D	E311 IB	1	0	520	2.107	0.865	1.00
12	D	E311 IB	13	12000	12520	1.313	1.145	1.30
13	D	E311 IB	14	13000	13520	1.294	1.076	1.45
14	D	E311 IB	24	23000	23520	1.212	1.038	1.66
15	D	E311 IB	55	54000	54600	1.628	1.213	1.04
16	D	E311 OB	18	17000	17520	1.538	0	1.06
17	D	E311 OB	19	18000	18520	2.238	0	1.16
18	D	E311 OB	20	19000	19520	1.700	0.873	1.14
19	D	E311 OB	46	45000	45520	1.224	1.077	1.29
20	D	E311 OB	53	52000	52600	1.169	1.257	0.86
21	C	E99 OB	4	3000	3500	2.19	2.60	2.58
22	C	E99 OB	5	4000	4500	2.57	2.50	1.37
23	C	E99 OB	6	5000	5500	2.18	2.50	2.12
24	C	E99 OB	10	9000	9500	1.93	1.76	2.11
25	C	E99 OB	12	11000	11500	1.93	2.28	1.91
26	C	E99 IB	6	5000	5500	2.03	2.40	2.72
27	C	E99 IB	7	6000	6500	1.58	1.61	2.85
28	C	E99 IB	8	7100	7600	2.40	2.49	1.56
29	C	E99 IB	11	10000	10500	2.01	2.37	2.40
30	C	E99 IB	12	11000	11500	2.03	2.67	1.42

A2 – Rutting Final Data Set:

No.	Terrain	Road	Section	Chainage		2013	2014	2017
				From	To	Avg Ruts	Avg Ruts	Avg Ruts
1	M	E18-1 IB	2	1000	1500	9.01	6.40	9.15
2	M	E18-1 IB	4	3000	3500	6.65	4.82	6.75
3	M	E18-1 IB	6	5000	5500	10.71	4.30	6.46
4	M	E18-1 IB	8	7000	7500	5.92	4.40	5.43
5	M	E18-1 IB	16	17500	18000	11.46	2.92	3.95
6	M	E18-1 IB	19	21000	21500	8.64	0.00	2.97
7	M	E18-1 OB	8	26500	27000	6.60	2.50	2.93
8	M	E18-1 OB	11	29500	30000	6.86	1.90	4.48
9	M	E18-2 OB	4	20800	21300	5.61	6.07	4.93
10	M	E18-2 IB	2	14500	14750	6.47	2.85	3.93
11	D	E311 IB	1	0	520	5.27	2.80	3.12
12	D	E311 IB	13	12000	12520	4.00	5.75	6.32
13	D	E311 IB	14	13000	13520	4.05	5.47	5.94
14	D	E311 IB	24	23000	23520	3.80	4.88	6.27
15	D	E311 IB	55	54000	54600	4.35	3.55	3.85
16	D	E311 OB	18	17000	17520	3.30	0.00	5.17
17	D	E311 OB	19	18000	18520	3.20	0.00	6.64
18	D	E311 OB	20	19000	19520	3.25	1.15	6.84
19	D	E311 OB	46	45000	45520	4.22	5.35	5.64
20	D	E311 OB	53	52000	52600	3.00	4.77	5.06
21	C	E99 OB	4	3000	3500	4.75	6.45	5.53
22	C	E99 OB	5	4000	4500	10.35	8.98	3.72
23	C	E99 OB	6	5000	5500	4.00	2.15	4.30
24	C	E99 OB	10	9000	9500	6.88	3.79	4.82
25	C	E99 OB	12	11000	11500	4.40	2.37	4.39
26	C	E99 IB	6	5000	5500	1.48	1.60	4.08
27	C	E99 IB	7	6000	6500	1.46	2.07	4.85
28	C	E99 IB	8	7100	7600	2.92	2.35	3.07
29	C	E99 IB	11	10000	10500	2.95	4.35	7.27
30	C	E99 IB	12	11000	11500	5.05	9.05	3.73



A3 - Cracking Data Set:

Road	Section	Chainage		2013			2014			2017		
		From	To	TB	TL	P	TB	TL	P	TL	TL	P
E18-1 IB	2	1000	1500	93.0	0.0	1	0	0	0	0	0.01	0
E18-1 IB	4	3000	3500	80.17	0.00	4	0	0	0	0	0.04	0
E18-1 IB	6	5000	5500	86.6	0.00	1	0	0	0	0	0.03	0
E18-1 IB	8	7000	7500	52.5	0.00	0	0	0	0	0	0.01	0
E18-1 IB	16	17500	18000	66.24	0.00	2	1.55	1.13	0	0	0.02	0
E18-1 IB	19	21000	21500	72.9	0.00	2	0	0	0	0	0.02	0
E18-1 OB	8	26500	27000	48.5	0	1	0	0	0	0	0	0
E18-1 OB	11	29500	30000	33.3	0	0	0	0	0	0	0	0
E18-2 OB	4	20800	21300	16.20	0.30	1	21	0	0	0	0.07	0
E18-2 IB	2	14500	14750	27.70	0.00	4	29.63	0	6	0	0	0
E311 IB	1	0	520	0	0	0	0	0	0	0	0.07	0
E311 IB	13	12000	12520	0.2	0	0	1	0	0	0	0	0
E311 IB	14	13000	13520	0	0	0	0	0	0	0	0	0
E311 IB	24	23000	23520	0	0	0	0	0	0	0	0	0
E311 IB	55	54000	54600	16.7	0	1	13.84	0	0	0	0	0
E311 OB	18	17000	17520	0.72	0.11	0	5	0	0	0	0	0
E311 OB	19	18000	18520	0.12	0	0	5	0	1	0	0	0
E311 OB	20	19000	19520	0	0	0	1.3	0	0	0	0.03	0
E311 OB	46	45000	45520	0.4	0	0	0.9	0	0	0	0.01	0
E311 OB	53	52000	52600	0	0	0	0	0	0	0	0	0
E99 OB	4	3000	3500	18.50	0	0	25.82	0	0	-	-	-
E99 OB	5	4000	4500	10.00	0	0	18.2	0	0	-	-	-
E99 OB	6	5000	5500	12.00	0	0	39.3	0	0	-	-	-
E99 OB	10	9000	9500	0.00	0	0	33.6	0	0	-	-	-
E99 OB	12	11000	11500	0.00	0	0	0	0	0	-	-	-
E99 IB	6	5000	5500	0.00	0	0	0.2	0.13	0	-	-	-
E99 IB	7	6000	6500	1.00	0.1	0	8.5	0	0	-	-	-
E99 IB	8	7100	7600	0.00	0	0	3.5	0	0	-	-	-
E99 IB	11	10000	10500	0.10	0	0	1.3	0	0	-	-	-
E99 IB	12	11000	11500	5.70	0	2	23.5	0	3	-	-	-

## Appendix B Material Properties

### MINISTRY OF INFRASTRUCTURE DEVELOPMENT MATERIAL PROPERTIES FOR ROAD WORKS

#### I. FORMATION

Type of Soil :

c. Dune Sand

- CBR @ 95% Compaction- < 15,
- Plasticity Index -Non plastic
- Maximum Dry Density – Around 1.69 to 1.75 Mg/M<sup>3</sup>

d. Gravel Material

- CBR @ 95% Compaction- >40
- Plasticity Index - <6
- Maximum Dry Density – 1.90 to 2.30 Mg/M<sup>3</sup>
- Compacted with optimum moisture to 98% of MDD

#### II. GRANULAR SUB BASE

Consists of hard durable natural or crushed stones free from clay and other deleterious material

- CBR @ 95% Compaction- >60%
- Liquid Limit – Max 35
- Plasticity Index - <6
- Maximum Dry Density – Min.2.10 Mg/M<sup>3</sup>
- Aggregate Soundness (MgSo<sub>4</sub>) – Max 12%
- Linear Shrinkage - Max 3%
- Chloride Content – Max 1%
- Sulphate Content – Max 0.5%

#### III. CEMENT STABILIZED SUB-BASE

Cement stabilized sub-base a mixture of coarse aggregate, fine aggregate, Cement and water. Coarse aggregate and fine aggregate cement and water are mixed in a calibrated mixing plant on a suitable proportion approved by the Engineer. The mixed cement stabilized sub base is discharged in a six wheel truck and transported to the laying area without losing the moisture. CSSB is laid on roadways which are completed with sub grade layer.

- Compressive Strength - 3.5 N/mm<sup>2</sup> at 28 days

#### IV. ASPHALT

Type of Asphalt Layer commonly used:

##### Base course & Wearing Course

Bituminous paving courses are a mixture of coarse aggregate, fine aggregate, filler material and bitumen binder (Grade 60/70). Coarse aggregate and fine aggregate including filler material are hot mixed in a calibrated mixing plant on a suitable proportion approved by the Engineer. The hot bitumen binder is then introduced into the mix in a proportion specified in the jobmix formula. The whole components are mixed for a specified period inside the mixer to obtain the final Homogeneous Asphalt mix. HMA is laid on roadways which are completed with Sub-base after the satisfactory application of prime coat.

##### a. Asphaltic Concrete Base Course

Bituminous base course is laid on the finished sub base layer after the satisfactory application of prime coat.

##### b. Asphaltic Concrete Wearing Course

Bituminous wearing course is laid on the base course layer after the satisfactory application of tack coat.

#### A. PROPERTIES OF MIX FOR ASPHALTIC CONCRETE

Properties	Bituminous Base Course	Bituminous Wearing Course
Number of compaction blow at each end of the specimen	75	75
Stability (Marshall ) Min. (N)	9800	11760
Flow (Marshall) mm in 0.25 units	8 -16	8 - 16
Stiffness, min. (N/0.25mm)	1225	1225
Percent Air Voids (VIM)	4 - 8	4 - 8
Percent Air Voids in Mineral aggregate, minimum % (VMA)	13	15
Percent Voids filled with Bitumen (VFB)	50 - 65	50 - 70
Loss of Marshall Stability in accordance with DM 405	Max. 25%	Max. 25%
Filler Bitumen Ratio	0.6 – 1.5	0.6 – 1.4

## B. AGGREGATE GRADING FOR ASPHALTIC CONCRETE

Sieve Size Square Opening ASTM (mm)	Bituminous Base Course	Bituminous Wearing Course
37.5	100	
25	80 – 100	100
19	62 – 92	86 – 100
12.5	-	69 – 87
9.5	45 – 75	58 – 75
4.75	30 – 55	40 – 60
2.36	20 – 40	25 – 45
0.850	15 – 30	15 – 30
0.425	10 - 22	10 - 22
0.180	6 - 15	6 - 15
0.075	2 - 8	2 - 8

Stabilising crushed material when tested in accordance with ASTM C136 shall have the following gradation:-

BS SIEVE	% PASSING
50mm	100
25mm	80-100
12.5mm	60-85
4.75mm	40-70
2.00mm	20-50
850 microns	15-25
425 microns	0-10
180 microns	0-2

